A Second-order and Two-scale Method in Cylindrical Coordinates for Mechanical Properties of Laminated Structure

Fei Han[1], Junzhi Cui[21], Yufeng Nie[1]

[1] *Department of Applied Mathematics, Northwestern Polytechnical University, Xi'an, 710072 China*
[2]*Academy of Mathematics and System Sciences, Chinese Academy of Sciences, Beijing, 100080 China*

Abstract A second-order and two-scale method is firstly presented in cylindrical coordinates, which is inspired by that the periodically laminated composite cylinder shows the periodicity characteristic in radial direction. This method is established for predicting mechanical properties of cylindrical structure, including stiffness parameters, strains, stresses and elastic limit loads. By defining four different operators and introducing an extended fourth-rank tensor, a uniform balance system of elasticity in cylindrical coordinates is expressed compactly. For this elastic model, the second-order and two-scale analysis formulations in cylindrical coordinates are developed by means of periodical material distribution in radial direction. Further, the second-order and two-scale expressions of the stains and stresses are derived for the hollow cylinders subject to uniform pressures and linearly varying pressures in axial direction, respectively, and the procedure of algorithms is described in detail. Finally, the numerical results for both typical structures are given, and compared with the results calculated by the software ANSYS. The agreements indicate that the second-order and two-scale method is effective and credible. It can be used to predict the mechanical performances of cylindrical structures.

Keywords: Multi-scale modeling; Cylindrical coordinates; Finite element analysis; Mechanical properties; Laminated cylinder

1. Introduction

Because the composites have complex micro-structures and heterogeneous parameters, it is difficult to predict the displacements, strains and stresses by the traditional finite element methods, due to the difficulty of generating FE meshes and the large computing capacity. In early 1970's, I.Babuska and J.L.Lions *et al*. presented the homogenization method for elastic structures of composites [1, 2]. And the homogenization method is effective to predict the effective parameters of composites, but not enough criterion for the strength of composites

---

1 Corresponding author. Tel.:+86 10 6256 8715; fax: +86 10 6254 2285
E-mail addresses: cjzgroup@mail.nwpu.edu.cn (F. Han), cjz@lsec.cc.ac.cn (J.Z. Cui)

since the method doesn't reflect the local strain and stress field of structures. After that, J.L.Lions, O.A.Oleinik, J.Z.Cui and L.Q.Cao *et al*. presented and developed the multi-scale analysis method to predict the physical and mechanical properties of composites [3-5]. The multi-scale analysis method reflects not only the global performance of structures and loads, but also the local behavior. And it can solve the difficult problem come from composites by computing the global structure and the local basic configuration respectively. However, the preceding methods were established in rectangular coordinates. Based on preceding works, a new multi-scale method in cylindrical coordinates is firstly established and applied to predict mechanical performance of composite cylindrical structures.

With the development of composites, the Laminated Composite Cylindrical Structure (LCCS for short) is extensively applied to a variety of engineering and industrial products, such as aircraft, aerospace, oil and gas pipeline and pressure vessel, etc, because of its low weight, high reliability, safe failure mode and other advantages. Most of LCCSs are made by repeatedly arranging a group of laminas with different ply angles and/or materials, which can be seen as a periodical arrangement. This kind of composite structure is called periodically laminated composite cylinder. This cylinder has a lot of thin laminas, so it is difficult to predict the mechanical performances by traditional numerical methods. Moreover, this kind of structure shows the periodicity characteristic only in radial direction. Considering above reasons, the Second-order and Two-scale Method in Cylindrical Coordinates (STMCC for short) is established in this paper based on homogenization theory.

The rest of this paper is organized as follows: In Section 2, the mathematical models of LCCS are presented, including geometrical model and basic equations. The second-order and two-scale analysis formulation for mechanical behaviors of composite cylinders is given in Section 3. Section 4 is devoted to the expansions on the strain and stress tensors for two kinds of typical axis-symmetric cylindrical structures. In Section 5, the procedure of STMCC based on FEM is stated. And the numerical results for mechanical behaviors of LCCS in different loading conditions are shown, and compared with the results calculated by ANSYS software in Section 6.

2. Mathematical model

2.1 Geometrical model

The geometrical model of LCCS is defined firstly, the inner radius is r_0, the outer radius is r_1, and $r_1 > r_0 > 0$. This LCCS is made by repeatedly arranging a group of laminas in radial direction. A basic configuration layer is composed by some thin laminas with different ply angles and/or materials, its thickness is ε, where $\varepsilon << |r_1 - r_0|$. In every basic configuration of LCCS, the arrangement of laminas is the same, shown in Fig. 1.

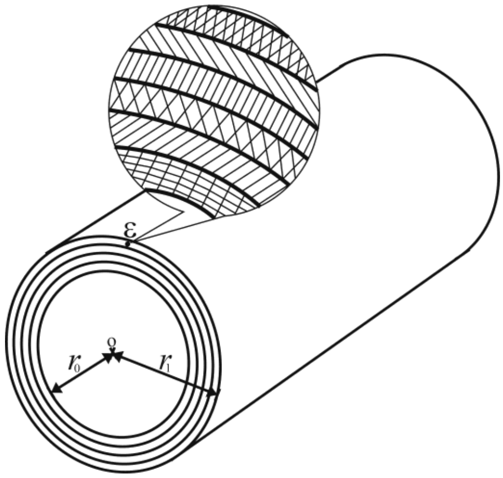

Fig. 1. A geometrical model of LCCS

2.2 Basic equations of elasticity in cylindrical coordinates

Stress Balance Equation:

$$\begin{cases} \dfrac{\partial \sigma_r}{\partial r} + \dfrac{1}{r}\dfrac{\partial \tau_{r\theta}}{\partial \theta} + \dfrac{\partial \tau_{zr}}{\partial z} + \dfrac{\sigma_r - \sigma_\theta}{r} + f_r = 0 \\ \dfrac{\partial \tau_{r\theta}}{\partial r} + \dfrac{1}{r}\dfrac{\partial \sigma_\theta}{\partial \theta} + \dfrac{\partial \tau_{\theta z}}{\partial z} + 2\dfrac{\tau_{r\theta}}{r} + f_\theta = 0 \\ \dfrac{\partial \tau_{zr}}{\partial r} + \dfrac{1}{r}\dfrac{\partial \tau_{\theta z}}{\partial \theta} + \dfrac{\partial \sigma_z}{\partial z} + \dfrac{\tau_{zr}}{r} + f_z = 0 \end{cases} \tag{1}$$

Geometry Equation:

$$
\begin{cases}
\varepsilon_r = \dfrac{\partial u_r^\varepsilon}{\partial r}; & \gamma_{r\theta} = \dfrac{1}{r}\dfrac{\partial u_r^\varepsilon}{\partial \theta} + \dfrac{\partial u_\theta^\varepsilon}{\partial r} - \dfrac{u_\theta^\varepsilon}{r} \\
\varepsilon_\theta = \dfrac{1}{r}\dfrac{\partial u_\theta^\varepsilon}{\partial \theta} + \dfrac{u_r^\varepsilon}{r}; & \gamma_{\theta z} = \dfrac{\partial u_\theta^\varepsilon}{\partial z} + \dfrac{1}{r}\dfrac{\partial u_z^\varepsilon}{\partial \theta} \\
\varepsilon_z = \dfrac{\partial u_z^\varepsilon}{\partial z}; & \gamma_{zr} = \dfrac{\partial u_z^\varepsilon}{\partial r} + \dfrac{\partial u_r^\varepsilon}{\partial z}
\end{cases} \tag{2}
$$

Constitutive Equation:

$$
\sigma_i = c_{ij}^\varepsilon \varepsilon_j \tag{3}
$$

where $i, j = 1,2,\cdots,6$, $(\sigma_1,\sigma_2,\sigma_3,\sigma_4,\sigma_5,\sigma_6) = (\sigma_r,\sigma_\theta,\sigma_z,\tau_{r\theta},\tau_{\theta z},\tau_{zr})$,

$(\varepsilon_1,\varepsilon_2,\varepsilon_3,\varepsilon_4,\varepsilon_5,\varepsilon_6) = (\varepsilon_r,\varepsilon_\theta,\varepsilon_z,\gamma_{r\theta},\gamma_{\theta z},\gamma_{zr})$.

According to (3) and (2), the equation (1) becomes the following equations with respect to the displacement:

$$
\begin{aligned}
&\frac{\partial}{\partial r}\Bigg[c_{11}^\varepsilon(r)\frac{\partial u_r^\varepsilon}{\partial r} + c_{12}^\varepsilon(r)\left(\frac{1}{r}\frac{\partial u_\theta^\varepsilon}{\partial \theta} + \frac{u_r^\varepsilon}{r}\right) + c_{13}^\varepsilon(r)\frac{\partial u_z^\varepsilon}{\partial z} + c_{14}^\varepsilon(r)\left(\frac{1}{r}\frac{\partial u_r^\varepsilon}{\partial \theta} + \frac{\partial u_\theta^\varepsilon}{\partial r} - \frac{u_\theta^\varepsilon}{r}\right) \\
&\quad + c_{15}^\varepsilon(r)\left(\frac{\partial u_\theta^\varepsilon}{\partial z} + \frac{1}{r}\frac{\partial u_z^\varepsilon}{\partial \theta}\right) + c_{16}^\varepsilon(r)\left(\frac{\partial u_z^\varepsilon}{\partial r} + \frac{\partial u_r^\varepsilon}{\partial z}\right) + 0\cdot\frac{u_z^\varepsilon}{r}\Bigg] + \\
&\frac{1}{r}\frac{\partial}{\partial \theta}\Bigg[c_{41}^\varepsilon(r)\frac{\partial u_r^\varepsilon}{\partial r} + c_{42}^\varepsilon(r)\left(\frac{1}{r}\frac{\partial u_\theta^\varepsilon}{\partial \theta} + \frac{u_r^\varepsilon}{r}\right) + c_{43}^\varepsilon(r)\frac{\partial u_z^\varepsilon}{\partial z} + c_{44}^\varepsilon(r)\left(\frac{1}{r}\frac{\partial u_r^\varepsilon}{\partial \theta} + \frac{\partial u_\theta^\varepsilon}{\partial r} - \frac{u_\theta^\varepsilon}{r}\right) \\
&\quad + c_{45}^\varepsilon(r)\left(\frac{\partial u_\theta^\varepsilon}{\partial z} + \frac{1}{r}\frac{\partial u_z^\varepsilon}{\partial \theta}\right) + c_{46}^\varepsilon(r)\left(\frac{\partial u_z^\varepsilon}{\partial r} + \frac{\partial u_r^\varepsilon}{\partial z}\right) + 0\cdot\frac{u_z^\varepsilon}{r}\Bigg] + \\
&\frac{\partial}{\partial z}\Bigg[c_{61}^\varepsilon(r)\frac{\partial u_r^\varepsilon}{\partial r} + c_{62}^\varepsilon(r)\left(\frac{1}{r}\frac{\partial u_\theta^\varepsilon}{\partial \theta} + \frac{u_r^\varepsilon}{r}\right) + c_{63}^\varepsilon(r)\frac{\partial u_z^\varepsilon}{\partial z} + c_{64}^\varepsilon(r)\left(\frac{1}{r}\frac{\partial u_r^\varepsilon}{\partial \theta} + \frac{\partial u_\theta^\varepsilon}{\partial r} - \frac{u_\theta^\varepsilon}{r}\right) \\
&\quad + c_{65}^\varepsilon(r)\left(\frac{\partial u_\theta^\varepsilon}{\partial z} + \frac{1}{r}\frac{\partial u_z^\varepsilon}{\partial \theta}\right) + c_{66}^\varepsilon(r)\left(\frac{\partial u_z^\varepsilon}{\partial r} + \frac{\partial u_r^\varepsilon}{\partial z}\right) + 0\cdot\frac{u_z^\varepsilon}{r}\Bigg] + \\
&\frac{1}{r}\Bigg[\left(c_{11}^\varepsilon(r) - c_{21}^\varepsilon(r)\right)\frac{\partial u_r^\varepsilon}{\partial r} + \left(c_{12}^\varepsilon(r) - c_{22}^\varepsilon(r)\right)\left(\frac{1}{r}\frac{\partial u_\theta^\varepsilon}{\partial \theta} + \frac{u_r^\varepsilon}{r}\right) + \left(c_{13}^\varepsilon(r) - c_{23}^\varepsilon(r)\right)\frac{\partial u_z^\varepsilon}{\partial z} \\
&\quad + \left(c_{14}^\varepsilon(r) - c_{24}^\varepsilon(r)\right)\left(\frac{1}{r}\frac{\partial u_r^\varepsilon}{\partial \theta} + \frac{\partial u_\theta^\varepsilon}{\partial r} - \frac{u_\theta^\varepsilon}{r}\right) + \left(c_{15}^\varepsilon(r) - c_{25}^\varepsilon(r)\right)\left(\frac{\partial u_\theta^\varepsilon}{\partial z} + \frac{1}{r}\frac{\partial u_z^\varepsilon}{\partial \theta}\right) \\
&\quad + \left(c_{16}^\varepsilon(r) - c_{26}^\varepsilon(r)\right)\left(\frac{\partial u_z^\varepsilon}{\partial r} + \frac{\partial u_r^\varepsilon}{\partial z}\right) + 0\cdot\frac{u_z^\varepsilon}{r}\Bigg] + f_r = 0
\end{aligned} \tag{4}
$$

$$\frac{\partial}{\partial r}\left[c_{41}^{\varepsilon}(r)\frac{\partial u_r^{\varepsilon}}{\partial r}+c_{42}^{\varepsilon}(r)\left(\frac{1}{r}\frac{\partial u_\theta^{\varepsilon}}{\partial\theta}+\frac{u_r^{\varepsilon}}{r}\right)+c_{43}^{\varepsilon}(r)\frac{\partial u_z^{\varepsilon}}{\partial z}+c_{44}^{\varepsilon}(r)\left(\frac{1}{r}\frac{\partial u_r^{\varepsilon}}{\partial\theta}+\frac{\partial u_\theta^{\varepsilon}}{\partial r}-\frac{u_\theta^{\varepsilon}}{r}\right)\right.$$

$$\left.+c_{45}^{\varepsilon}(r)\left(\frac{\partial u_\theta^{\varepsilon}}{\partial z}+\frac{1}{r}\frac{\partial u_z^{\varepsilon}}{\partial\theta}\right)+c_{46}^{\varepsilon}(r)\left(\frac{\partial u_z^{\varepsilon}}{\partial r}+\frac{\partial u_r^{\varepsilon}}{\partial z}\right)+0\cdot\frac{u_z^{\varepsilon}}{r}\right]+$$

$$\frac{1}{r}\frac{\partial}{\partial\theta}\left[c_{21}^{\varepsilon}(r)\frac{\partial u_r^{\varepsilon}}{\partial r}+c_{22}^{\varepsilon}(r)\left(\frac{1}{r}\frac{\partial u_\theta^{\varepsilon}}{\partial\theta}+\frac{u_r^{\varepsilon}}{r}\right)+c_{23}^{\varepsilon}(r)\frac{\partial u_z^{\varepsilon}}{\partial z}+c_{24}^{\varepsilon}(r)\left(\frac{1}{r}\frac{\partial u_r^{\varepsilon}}{\partial\theta}+\frac{\partial u_\theta^{\varepsilon}}{\partial r}-\frac{u_\theta^{\varepsilon}}{r}\right)\right.$$

$$\left.+c_{25}^{\varepsilon}(r)\left(\frac{\partial u_\theta^{\varepsilon}}{\partial z}+\frac{1}{r}\frac{\partial u_z^{\varepsilon}}{\partial\theta}\right)+c_{26}^{\varepsilon}(r)\left(\frac{\partial u_z^{\varepsilon}}{\partial r}+\frac{\partial u_r^{\varepsilon}}{\partial z}\right)+0\cdot\frac{u_z^{\varepsilon}}{r}\right]+$$

$$\frac{\partial}{\partial z}\left[c_{51}^{\varepsilon}(r)\frac{\partial u_r^{\varepsilon}}{\partial r}+c_{52}^{\varepsilon}(r)\left(\frac{1}{r}\frac{\partial u_\theta^{\varepsilon}}{\partial\theta}+\frac{u_r^{\varepsilon}}{r}\right)+c_{53}^{\varepsilon}(r)\frac{\partial u_z^{\varepsilon}}{\partial z}+c_{54}^{\varepsilon}(r)\left(\frac{1}{r}\frac{\partial u_r^{\varepsilon}}{\partial\theta}+\frac{\partial u_\theta^{\varepsilon}}{\partial r}-\frac{u_\theta^{\varepsilon}}{r}\right)\right.$$

$$\left.+c_{55}^{\varepsilon}(r)\left(\frac{\partial u_\theta^{\varepsilon}}{\partial z}+\frac{1}{r}\frac{\partial u_z^{\varepsilon}}{\partial\theta}\right)+c_{56}^{\varepsilon}(r)\left(\frac{\partial u_z^{\varepsilon}}{\partial r}+\frac{\partial u_r^{\varepsilon}}{\partial z}\right)+0\cdot\frac{u_z^{\varepsilon}}{r}\right]+$$

$$\frac{1}{r}\left[2c_{41}^{\varepsilon}(r)\frac{\partial u_r^{\varepsilon}}{\partial r}+2c_{42}^{\varepsilon}(r)\left(\frac{1}{r}\frac{\partial u_\theta^{\varepsilon}}{\partial\theta}+\frac{u_r^{\varepsilon}}{r}\right)+2c_{43}^{\varepsilon}(r)\frac{\partial u_z^{\varepsilon}}{\partial z}+2c_{44}^{\varepsilon}(r)\left(\frac{1}{r}\frac{\partial u_r^{\varepsilon}}{\partial\theta}+\frac{\partial u_\theta^{\varepsilon}}{\partial r}-\frac{u_\theta^{\varepsilon}}{r}\right)\right.$$

$$\left.+2c_{45}^{\varepsilon}(r)\left(\frac{\partial u_\theta^{\varepsilon}}{\partial z}+\frac{1}{r}\frac{\partial u_z^{\varepsilon}}{\partial\theta}\right)+2c_{46}^{\varepsilon}(r)\left(\frac{\partial u_z^{\varepsilon}}{\partial r}+\frac{\partial u_r^{\varepsilon}}{\partial z}\right)+0\cdot\frac{u_z^{\varepsilon}}{r}\right]+f_\theta=0 \tag{5}$$

$$\frac{\partial}{\partial r}\left[c_{61}^{\varepsilon}(r)\frac{\partial u_r^{\varepsilon}}{\partial r}+c_{62}^{\varepsilon}(r)\left(\frac{1}{r}\frac{\partial u_\theta^{\varepsilon}}{\partial\theta}+\frac{u_r^{\varepsilon}}{r}\right)+c_{63}^{\varepsilon}(r)\frac{\partial u_z^{\varepsilon}}{\partial z}+c_{64}^{\varepsilon}(r)\left(\frac{1}{r}\frac{\partial u_r^{\varepsilon}}{\partial\theta}+\frac{\partial u_\theta^{\varepsilon}}{\partial r}-\frac{u_\theta^{\varepsilon}}{r}\right)\right.$$

$$\left.+c_{65}^{\varepsilon}(r)\left(\frac{\partial u_\theta^{\varepsilon}}{\partial z}+\frac{1}{r}\frac{\partial u_z^{\varepsilon}}{\partial\theta}\right)+c_{66}^{\varepsilon}(r)\left(\frac{\partial u_z^{\varepsilon}}{\partial r}+\frac{\partial u_r^{\varepsilon}}{\partial z}\right)+0\cdot\frac{u_z^{\varepsilon}}{r}\right]+$$

$$\frac{1}{r}\frac{\partial}{\partial\theta}\left[c_{51}^{\varepsilon}(r)\frac{\partial u_r^{\varepsilon}}{\partial r}+c_{52}^{\varepsilon}(r)\left(\frac{1}{r}\frac{\partial u_\theta^{\varepsilon}}{\partial\theta}+\frac{u_r^{\varepsilon}}{r}\right)+c_{53}^{\varepsilon}(r)\frac{\partial u_z^{\varepsilon}}{\partial z}+c_{54}^{\varepsilon}(r)\left(\frac{1}{r}\frac{\partial u_r^{\varepsilon}}{\partial\theta}+\frac{\partial u_\theta^{\varepsilon}}{\partial r}-\frac{u_\theta^{\varepsilon}}{r}\right)\right.$$

$$\left.+c_{55}^{\varepsilon}(r)\left(\frac{\partial u_\theta^{\varepsilon}}{\partial z}+\frac{1}{r}\frac{\partial u_z^{\varepsilon}}{\partial\theta}\right)+c_{56}^{\varepsilon}(r)\left(\frac{\partial u_z^{\varepsilon}}{\partial r}+\frac{\partial u_r^{\varepsilon}}{\partial z}\right)+0\cdot\frac{u_z^{\varepsilon}}{r}\right]+$$

$$\frac{\partial}{\partial z}\left[c_{31}^{\varepsilon}(r)\frac{\partial u_r^{\varepsilon}}{\partial r}+c_{32}^{\varepsilon}(r)\left(\frac{1}{r}\frac{\partial u_\theta^{\varepsilon}}{\partial\theta}+\frac{u_r^{\varepsilon}}{r}\right)+c_{33}^{\varepsilon}(r)\frac{\partial u_z^{\varepsilon}}{\partial z}+c_{34}^{\varepsilon}(r)\left(\frac{1}{r}\frac{\partial u_r^{\varepsilon}}{\partial\theta}+\frac{\partial u_\theta^{\varepsilon}}{\partial r}-\frac{u_\theta^{\varepsilon}}{r}\right)\right.$$

$$\left.+c_{35}^{\varepsilon}(r)\left(\frac{\partial u_\theta^{\varepsilon}}{\partial z}+\frac{1}{r}\frac{\partial u_z^{\varepsilon}}{\partial\theta}\right)+c_{36}^{\varepsilon}(r)\left(\frac{\partial u_z^{\varepsilon}}{\partial r}+\frac{\partial u_r^{\varepsilon}}{\partial z}\right)+0\cdot\frac{u_z^{\varepsilon}}{r}\right]+$$

$$\frac{1}{r}\left[c_{61}^{\varepsilon}(r)\frac{\partial u_r^{\varepsilon}}{\partial r}+c_{62}^{\varepsilon}(r)\left(\frac{1}{r}\frac{\partial u_\theta^{\varepsilon}}{\partial\theta}+\frac{u_r^{\varepsilon}}{r}\right)+c_{63}^{\varepsilon}(r)\frac{\partial u_z^{\varepsilon}}{\partial z}+c_{64}^{\varepsilon}(r)\left(\frac{1}{r}\frac{\partial u_r^{\varepsilon}}{\partial\theta}+\frac{\partial u_\theta^{\varepsilon}}{\partial r}-\frac{u_\theta^{\varepsilon}}{r}\right)\right.$$

$$\left.+c_{65}^{\varepsilon}(r)\left(\frac{\partial u_\theta^{\varepsilon}}{\partial z}+\frac{1}{r}\frac{\partial u_z^{\varepsilon}}{\partial\theta}\right)+c_{66}^{\varepsilon}(r)\left(\frac{\partial u_z^{\varepsilon}}{\partial r}+\frac{\partial u_r^{\varepsilon}}{\partial z}\right)+0\cdot\frac{u_z^{\varepsilon}}{r}\right]+f_z=0 \tag{6}$$

Define $\Psi_1=\frac{\partial}{\partial r},\Psi_2=\frac{1}{r}\frac{\partial}{\partial\theta},\Psi_3=\frac{\partial}{\partial z},\Psi_4=\frac{1}{r}$, then the above three equations are rewritten as follows

$$\Psi_j\left(a^{\varepsilon}_{ijhk}(r)\Psi_k(u^{\varepsilon}_h)\right)+f_i=0 \tag{7}$$

where $i,h=1,2,3$, $j,k=1,2,3,4$ and $u^{\varepsilon}_1,u^{\varepsilon}_2,u^{\varepsilon}_3$ represent u^{ε}_r, u^{ε}_{θ} and u^{ε}_z respectively. The coefficient tensors a^{ε}_{ijhk} correspond to the constitutive parameters c^{ε}_{ij}. From (4) to (7), the following correspondence is obtained

$$a^{\varepsilon}_{ijhk}=\begin{bmatrix}
a^{\varepsilon}_{1111} & a^{\varepsilon}_{1122} & a^{\varepsilon}_{1133} & a^{\varepsilon}_{1112} & a^{\varepsilon}_{1123} & a^{\varepsilon}_{1131} & a^{\varepsilon}_{1121} & a^{\varepsilon}_{1132} & a^{\varepsilon}_{1113} & a^{\varepsilon}_{1114} & a^{\varepsilon}_{1124} & a^{\varepsilon}_{1134}\\
a^{\varepsilon}_{2211} & a^{\varepsilon}_{2222} & a^{\varepsilon}_{2233} & a^{\varepsilon}_{2212} & a^{\varepsilon}_{2223} & a^{\varepsilon}_{2231} & a^{\varepsilon}_{2221} & a^{\varepsilon}_{2232} & a^{\varepsilon}_{2213} & a^{\varepsilon}_{2214} & a^{\varepsilon}_{2224} & a^{\varepsilon}_{2234}\\
a^{\varepsilon}_{3311} & a^{\varepsilon}_{3322} & a^{\varepsilon}_{3333} & a^{\varepsilon}_{3312} & a^{\varepsilon}_{3323} & a^{\varepsilon}_{3331} & a^{\varepsilon}_{3321} & a^{\varepsilon}_{3332} & a^{\varepsilon}_{3313} & a^{\varepsilon}_{3314} & a^{\varepsilon}_{3324} & a^{\varepsilon}_{3334}\\
a^{\varepsilon}_{1211} & a^{\varepsilon}_{1222} & a^{\varepsilon}_{1233} & a^{\varepsilon}_{1212} & a^{\varepsilon}_{1223} & a^{\varepsilon}_{1231} & a^{\varepsilon}_{1221} & a^{\varepsilon}_{1232} & a^{\varepsilon}_{1213} & a^{\varepsilon}_{1214} & a^{\varepsilon}_{1224} & a^{\varepsilon}_{1234}\\
a^{\varepsilon}_{2311} & a^{\varepsilon}_{2322} & a^{\varepsilon}_{2333} & a^{\varepsilon}_{2312} & a^{\varepsilon}_{2323} & a^{\varepsilon}_{2331} & a^{\varepsilon}_{2321} & a^{\varepsilon}_{2332} & a^{\varepsilon}_{2313} & a^{\varepsilon}_{2314} & a^{\varepsilon}_{2324} & a^{\varepsilon}_{2334}\\
a^{\varepsilon}_{3111} & a^{\varepsilon}_{3122} & a^{\varepsilon}_{3133} & a^{\varepsilon}_{3112} & a^{\varepsilon}_{3123} & a^{\varepsilon}_{3131} & a^{\varepsilon}_{3121} & a^{\varepsilon}_{3132} & a^{\varepsilon}_{3113} & a^{\varepsilon}_{3114} & a^{\varepsilon}_{3124} & a^{\varepsilon}_{3134}\\
a^{\varepsilon}_{2111} & a^{\varepsilon}_{2122} & a^{\varepsilon}_{2133} & a^{\varepsilon}_{2112} & a^{\varepsilon}_{2123} & a^{\varepsilon}_{2131} & a^{\varepsilon}_{2121} & a^{\varepsilon}_{2132} & a^{\varepsilon}_{2113} & a^{\varepsilon}_{2114} & a^{\varepsilon}_{2124} & a^{\varepsilon}_{2134}\\
a^{\varepsilon}_{3211} & a^{\varepsilon}_{3222} & a^{\varepsilon}_{3233} & a^{\varepsilon}_{3212} & a^{\varepsilon}_{3223} & a^{\varepsilon}_{3231} & a^{\varepsilon}_{3221} & a^{\varepsilon}_{3232} & a^{\varepsilon}_{3213} & a^{\varepsilon}_{3214} & a^{\varepsilon}_{3224} & a^{\varepsilon}_{3234}\\
a^{\varepsilon}_{1311} & a^{\varepsilon}_{1322} & a^{\varepsilon}_{1333} & a^{\varepsilon}_{1312} & a^{\varepsilon}_{1323} & a^{\varepsilon}_{1331} & a^{\varepsilon}_{1321} & a^{\varepsilon}_{1332} & a^{\varepsilon}_{1313} & a^{\varepsilon}_{1314} & a^{\varepsilon}_{1324} & a^{\varepsilon}_{1334}\\
a^{\varepsilon}_{1411} & a^{\varepsilon}_{1422} & a^{\varepsilon}_{1433} & a^{\varepsilon}_{1412} & a^{\varepsilon}_{1423} & a^{\varepsilon}_{1431} & a^{\varepsilon}_{1421} & a^{\varepsilon}_{1432} & a^{\varepsilon}_{1413} & a^{\varepsilon}_{1414} & a^{\varepsilon}_{1424} & a^{\varepsilon}_{1434}\\
a^{\varepsilon}_{2411} & a^{\varepsilon}_{2422} & a^{\varepsilon}_{2433} & a^{\varepsilon}_{2412} & a^{\varepsilon}_{2423} & a^{\varepsilon}_{2431} & a^{\varepsilon}_{2421} & a^{\varepsilon}_{2432} & a^{\varepsilon}_{2413} & a^{\varepsilon}_{2414} & a^{\varepsilon}_{2424} & a^{\varepsilon}_{2434}\\
a^{\varepsilon}_{3411} & a^{\varepsilon}_{3422} & a^{\varepsilon}_{3433} & a^{\varepsilon}_{3412} & a^{\varepsilon}_{3423} & a^{\varepsilon}_{3431} & a^{\varepsilon}_{3421} & a^{\varepsilon}_{3432} & a^{\varepsilon}_{3413} & a^{\varepsilon}_{3414} & a^{\varepsilon}_{3424} & a^{\varepsilon}_{3434}
\end{bmatrix}$$

$$=\begin{bmatrix}
c^{\varepsilon}_{11} & c^{\varepsilon}_{12} & c^{\varepsilon}_{13} & c^{\varepsilon}_{14} & c^{\varepsilon}_{15} & c^{\varepsilon}_{16} & c^{\varepsilon}_{14} & c^{\varepsilon}_{15} & c^{\varepsilon}_{16} & c^{\varepsilon}_{12} & -c^{\varepsilon}_{14} & 0\\
c^{\varepsilon}_{21} & c^{\varepsilon}_{22} & c^{\varepsilon}_{23} & c^{\varepsilon}_{24} & c^{\varepsilon}_{25} & c^{\varepsilon}_{26} & c^{\varepsilon}_{24} & c^{\varepsilon}_{25} & c^{\varepsilon}_{26} & c^{\varepsilon}_{22} & -c^{\varepsilon}_{24} & 0\\
c^{\varepsilon}_{31} & c^{\varepsilon}_{32} & c^{\varepsilon}_{33} & c^{\varepsilon}_{34} & c^{\varepsilon}_{35} & c^{\varepsilon}_{36} & c^{\varepsilon}_{34} & c^{\varepsilon}_{35} & c^{\varepsilon}_{36} & c^{\varepsilon}_{32} & -c^{\varepsilon}_{34} & 0\\
c^{\varepsilon}_{41} & c^{\varepsilon}_{42} & c^{\varepsilon}_{43} & c^{\varepsilon}_{44} & c^{\varepsilon}_{45} & c^{\varepsilon}_{46} & c^{\varepsilon}_{44} & c^{\varepsilon}_{45} & c^{\varepsilon}_{46} & c^{\varepsilon}_{42} & -c^{\varepsilon}_{44} & 0\\
c^{\varepsilon}_{51} & c^{\varepsilon}_{52} & c^{\varepsilon}_{53} & c^{\varepsilon}_{54} & c^{\varepsilon}_{55} & c^{\varepsilon}_{56} & c^{\varepsilon}_{54} & c^{\varepsilon}_{55} & c^{\varepsilon}_{56} & c^{\varepsilon}_{52} & -c^{\varepsilon}_{54} & 0\\
c^{\varepsilon}_{61} & c^{\varepsilon}_{62} & c^{\varepsilon}_{63} & c^{\varepsilon}_{64} & c^{\varepsilon}_{65} & c^{\varepsilon}_{66} & c^{\varepsilon}_{64} & c^{\varepsilon}_{65} & c^{\varepsilon}_{66} & c^{\varepsilon}_{62} & -c^{\varepsilon}_{64} & 0\\
c^{\varepsilon}_{41} & c^{\varepsilon}_{42} & c^{\varepsilon}_{43} & c^{\varepsilon}_{44} & c^{\varepsilon}_{45} & c^{\varepsilon}_{46} & c^{\varepsilon}_{44} & c^{\varepsilon}_{45} & c^{\varepsilon}_{46} & c^{\varepsilon}_{42} & -c^{\varepsilon}_{44} & 0\\
c^{\varepsilon}_{51} & c^{\varepsilon}_{52} & c^{\varepsilon}_{53} & c^{\varepsilon}_{54} & c^{\varepsilon}_{55} & c^{\varepsilon}_{56} & c^{\varepsilon}_{54} & c^{\varepsilon}_{55} & c^{\varepsilon}_{56} & c^{\varepsilon}_{52} & -c^{\varepsilon}_{54} & 0\\
c^{\varepsilon}_{61} & c^{\varepsilon}_{62} & c^{\varepsilon}_{63} & c^{\varepsilon}_{64} & c^{\varepsilon}_{65} & c^{\varepsilon}_{66} & c^{\varepsilon}_{64} & c^{\varepsilon}_{65} & c^{\varepsilon}_{66} & c^{\varepsilon}_{62} & -c^{\varepsilon}_{64} & 0\\
d^{\varepsilon}_{11} & d^{\varepsilon}_{12} & d^{\varepsilon}_{13} & d^{\varepsilon}_{14} & d^{\varepsilon}_{15} & d^{\varepsilon}_{16} & d^{\varepsilon}_{14} & d^{\varepsilon}_{15} & d^{\varepsilon}_{16} & d^{\varepsilon}_{12} & -d^{\varepsilon}_{14} & 0\\
d^{\varepsilon}_{21} & d^{\varepsilon}_{22} & d^{\varepsilon}_{23} & d^{\varepsilon}_{24} & d^{\varepsilon}_{25} & d^{\varepsilon}_{26} & d^{\varepsilon}_{24} & d^{\varepsilon}_{25} & d^{\varepsilon}_{26} & d^{\varepsilon}_{22} & -d^{\varepsilon}_{24} & 0\\
c^{\varepsilon}_{61} & c^{\varepsilon}_{62} & c^{\varepsilon}_{63} & c^{\varepsilon}_{64} & c^{\varepsilon}_{65} & c^{\varepsilon}_{66} & c^{\varepsilon}_{64} & c^{\varepsilon}_{65} & c^{\varepsilon}_{66} & c^{\varepsilon}_{62} & -c^{\varepsilon}_{64} & 0
\end{bmatrix} \tag{8}$$

where $a^{\varepsilon}_{ij34}(r)$ equal to zero and $d^{\varepsilon}_{1m}=c^{\varepsilon}_{1m}-c^{\varepsilon}_{2m}$, $d^{\varepsilon}_{2m}=2c^{\varepsilon}_{4m}$, $m=1,2,\cdots,6$.

3. Second-order and two-scale analysis formulation

For the periodically laminated cylindrical structure, the material is homogeneous in circumferential and axial direction, but periodical in radial direction. So, for the investigated structure Ω, $\Omega = \Omega_z \times \Omega_\theta \times \bigcup_{t \in Z} \varepsilon(Q_r + t)$, where Ω_z and Ω_θ respectively represent the range of θ and z in the whole cylindrical structure, and Q_r is unit cell in radial direction and $Q_r = [0,1]$.

We consider the following elasticity boundary value problem:

$$\begin{cases} A_\varepsilon^i \mathbf{u}^\varepsilon(r,\theta,z) = -\Psi_j\left(a_{ijhk}^\varepsilon(r)\Psi_k\left(u_h^\varepsilon(r,\theta,z)\right)\right) = f_i(r,\theta,z) & (r,\theta,z) \in \Omega \\ \mathbf{u}^\varepsilon(r,\theta,z) = 0 & (r,\theta,z) \in \Gamma_1 \\ \sigma(u) \equiv \nu_j a_{ijhk}^\varepsilon(r)\Psi_k\left(u_h^\varepsilon(r,\theta,z)\right) = p_i(r,\theta,z) & (r,\theta,z) \in \Gamma_2 \\ \left(\Gamma_1 \cap \Gamma_2 = 0,\ \Gamma_1 \cup \Gamma_2 = \partial\Omega\right) \end{cases} \tag{9}$$

It is temporarily supposed that there exist the homogeneous effective coefficient tensors $\{\hat{a}_{ijhk}\}$ in global Ω, where $i,h = 1,2,3$, $j,k = 1,2,3,4$. Further the vector-valued displacement $\mathbf{u}^0(r,\theta,z)$ is defined as the solution of the following homogenization problem:

$$\begin{cases} -\hat{a}_{ijhk}\Psi_j\left(\Psi_k\left(u_h^0(r,\theta,z)\right)\right) = f_i(r,\theta,z) & (r,\theta,z) \in \Omega \\ \mathbf{u}^0(r,\theta,z) = 0 & (r,\theta,z) \in \Gamma_1 \\ \sigma(u) \equiv \nu_j \hat{a}_{ijhk}\Psi_k\left(u_h^\varepsilon(r,\theta,z)\right) = p_i(r,\theta,z) & (r,\theta,z) \in \Gamma_2 \\ \left(\Gamma_1 \cap \Gamma_2 = 0,\ \Gamma_1 \cup \Gamma_2 = \partial\Omega\right) \end{cases} \tag{10}$$

We will give the computational formula on $\{\hat{a}_{ijhk}\}$ later.

Since the periodical basic cell of LCCS has ε thickness and there exists the periodicity only in radial direction, let $\xi = \frac{r - r_0}{\varepsilon}$ represents the local coordinate in Q_r. Then,

$$a_{ijhk}^\varepsilon(r) = a_{ijhk}\left(\frac{r - r_0}{\varepsilon}\right) = a_{ijhk}(\xi) \tag{11}$$

$$\mathbf{u}^\varepsilon(r,\theta,z) = \mathbf{u}(r,\xi,\theta,z) \tag{12}$$

Suppose that $\mathbf{u}^\varepsilon(r,\theta,z)$ is expanded into following form:

$$
\begin{aligned}
\mathbf{u}^{\varepsilon}(r,\theta,z) &= \mathbf{u}(r,\xi,\theta,z) \\
&= \mathbf{u}_0(r,\xi,\theta,z) + \varepsilon\mathbf{u}_1(r,\xi,\theta,z) + \varepsilon^2\mathbf{u}_2(r,\xi,\theta,z) + \varepsilon^3\mathbf{P}(r,\xi,\theta,z)
\end{aligned} \tag{13}
$$

Due to $\xi = \dfrac{r-r_0}{\varepsilon}$, respecting

$$
\frac{\partial u_h^{\varepsilon}}{\partial r} = \frac{\partial u_h}{\partial r} + \frac{1}{\varepsilon}\frac{\partial u_h}{\partial \xi}, \quad \frac{\partial u_h^{\varepsilon}}{\partial \theta} = \frac{\partial u_h}{\partial \theta}, \quad \frac{\partial u_h^{\varepsilon}}{\partial z} = \frac{\partial u_h}{\partial z} \tag{14}
$$

The following equality is obtained:

$$
\begin{aligned}
A_{\varepsilon}^{i} = &-\varepsilon^{-2}\frac{\partial}{\partial\xi}\left(a_{i1h1}(\xi)\frac{\partial}{\partial\xi}\right) - \varepsilon^{-1}\left[\frac{\partial}{\partial\xi}\left(a_{i1hk}(\xi)\Psi_k\right) + \Psi_j\left(a_{ijh1}(\xi)\frac{\partial}{\partial\xi}\right)\right] \\
&- \varepsilon^{0}\Psi_j\left(a_{ijhk}(\xi)\Psi_k\right)
\end{aligned} \tag{15}
$$

It also can be written as

$$
A_{\varepsilon}^{i} = \varepsilon^{-2}A_0^i + \varepsilon^{-1}A_1^i + \varepsilon^{0}A_2^i \tag{16}
$$

where

$$
\begin{cases}
A_0^i = -\dfrac{\partial}{\partial\xi}\left(a_{i1h1}(\xi)\dfrac{\partial}{\partial\xi}\right) \\
A_1^i = -\dfrac{\partial}{\partial\xi}\left(a_{i1hk}(\xi)\Psi_k\right) - \Psi_j\left(a_{ijh1}(\xi)\dfrac{\partial}{\partial\xi}\right) \\
A_2^i = -\Psi_j\left(a_{ijhk}(\xi)\Psi_k\right)
\end{cases} \tag{17}
$$

Substituting (13) and (16) into (9) one obtains the following equality:

$$
\begin{aligned}
A_{\varepsilon}^{i}\mathbf{u}^{\varepsilon} &= \left(\varepsilon^{-2}A_0^i + \varepsilon^{-1}A_1^i + \varepsilon^{0}A_2^i\right)\Big(\mathbf{u}_0(r,\xi,\theta,z) \\
&\quad + \varepsilon\mathbf{u}_1(r,\xi,\theta,z) + \varepsilon^2\mathbf{u}_2(r,\xi,\theta,z) + \varepsilon^3\mathbf{P}(r,\xi,\theta,z)\Big) \\
&= \varepsilon^{-2}A_0^i\mathbf{u}_0(r,\xi,\theta,z) + \varepsilon^{-1}\left(A_0^i\mathbf{u}_1(r,\xi,\theta,z) + A_1^i\mathbf{u}_0(r,\xi,\theta,z)\right) \\
&\quad + \varepsilon^{0}\left(A_0^i\mathbf{u}_2(r,\xi,\theta,z) + A_1^i\mathbf{u}_1(r,\xi,\theta,z) + A_2^i\mathbf{u}_0(r,\xi,\theta,z)\right) + \mathrm{O}(\varepsilon) \\
&= f_i(r,\theta,z)
\end{aligned} \tag{18}
$$

The equality (18) holds for any $\varepsilon > 0$. Firstly, by comparing the coefficients of ε^{-2} in both sides of equality (18), the following equation is obtained:

$$
A_0^i\mathbf{u}_0(r,\xi,\theta,z) = 0 \tag{19}
$$

The equation (19) has a special solution as follows

$$\mathbf{u}_0(r,\xi,\theta,z)=\mathbf{u}^0(r,\theta,z) \tag{20}$$

which only depends on macro-variable. Secondly, by comparing the coefficients of ε^{-1} in both sides of equality (18), the following equation is obtained:

$$A_0^i\mathbf{u}_1(r,\xi,\theta,z)+A_1^i\mathbf{u}^0(r,\theta,z)=0 \tag{21}$$

namely

$$-\frac{\partial}{\partial\xi}\left[a_{i1h1}(\xi)\frac{\partial u_{1,h}(r,\xi,\theta,z)}{\partial\xi}\right]=\frac{\partial a_{i1hk}(\xi)}{\partial\xi}\Psi_k\left(u_h^0(r,\theta,z)\right) \tag{22}$$

Let $\mathbf{N}_{\alpha_1}(\xi)$ is the solution of the following problem:

$$\begin{cases}\dfrac{\partial}{\partial\xi}\left(a_{i1h1}(\xi)\dfrac{\partial N_{\alpha_1 hm}(\xi)}{\partial\xi}\right)=-\dfrac{\partial a_{i1m\alpha_1}(\xi)}{\partial\xi} & \xi\in Q_r\\ N_{\alpha_1 hm}(\xi)=0 & \xi\in\partial Q_r\end{cases} \tag{23}$$

where $\mathbf{N}_{\alpha_1}(\xi)$ $(\alpha_1=1,2,3,4)$ are matrix valued functions in unit cell Q_r. It has the following forms

$$\mathbf{N}_{\alpha_1}(\xi)=\begin{pmatrix}N_{\alpha_1 11}(\xi) & N_{\alpha_1 12}(\xi) & N_{\alpha_1 13}(\xi)\\ N_{\alpha_1 21}(\xi) & N_{\alpha_1 22}(\xi) & N_{\alpha_1 23}(\xi)\\ N_{\alpha_1 31}(\xi) & N_{\alpha_1 32}(\xi) & N_{\alpha_1 33}(\xi)\end{pmatrix}$$

In terms of Lax-Milgram lemma, Korn’s inequality and the symmetry and regularity of the coefficient matrix $\{a_{i1h1}\}=\begin{bmatrix}c_{11} & c_{14} & c_{16}\\ c_{41} & c_{44} & c_{46}\\ c_{61} & c_{64} & c_{66}\end{bmatrix}$ obtained from (8), it is easy to prove that above problem (23) has the unique solution. Substituting (23) into (22) one obtains

$$\frac{\partial}{\partial\xi}\left[a_{i1h1}(\xi)\frac{\partial}{\partial\xi}\left(u_{1,h}(r,\xi,\theta,z)-N_{\alpha_1 hm}(\xi)\Psi_{\alpha_1}\left(u_m^0(r,\theta,z)\right)\right)\right]=0 \tag{24}$$

The equation (24) has a specific solution with the following form

$$\mathbf{u}_1(r,\xi,\theta,z)=\mathbf{N}_{\alpha_1}(\xi)\Psi_{\alpha_1}\left(\mathbf{u}^0(r,\theta,z)\right) \tag{25}$$

Inspired by [6, 7], let

$$\hat{a}_{ijhk} = \frac{1}{|Q_r|}\int_{Q_r}\left(a_{ijhk}(\xi) + a_{ijp1}(\xi)\frac{\partial N_{kph}(\xi)}{\partial \xi}\right)d\xi\,,\quad \xi \in Q_r \tag{26}$$

Since the right side of the equality (18) is independent on ε, let the coefficient of ε^0 in the left side of (18) equal to $f_i(r,\theta,z)$, that is

$$A_0^i \mathbf{u}_2(r,\xi,\theta,z) + A_1^i \mathbf{u}_1(r,\xi,\theta,z) + A_2^i \mathbf{u}^0(r,\xi,\theta,z) = f_i(r,\theta,z) \tag{27}$$

Substituting the expressions of A_0^i, A_1^i, A_2^i and $\mathbf{u}_1$ in (17) and (25), and homogenized equation (10) and homogenized coefficient (26) into (27), one obtains the following equality:

$$\begin{aligned}
-\frac{\partial}{\partial \xi}\left[a_{i1h1}(\xi)\frac{\partial u_{2,h}(r,\xi,\theta,z)}{\partial \xi}\right] &= \frac{\partial}{\partial \xi}\left(a_{i1hk}(\xi)N_{\alpha_1 hm}(\xi)\Psi_k \Psi_{\alpha_1}(u_m^0)\right) \\
&\quad + \Psi_j\left[a_{ijh1}(\xi)\frac{\partial N_{\alpha_1 hm}(\xi)}{\partial \xi}\Psi_{\alpha_1}(u_m^0)\right] + \Psi_j\left(a_{ijhk}(\xi)\Psi_k(u_h^0)\right) + f_i(r,\theta,z) \\
&= \frac{\partial}{\partial \xi}\left(a_{i1hk}(\xi)N_{\alpha_1 hm}(\xi)\right)\Psi_k \Psi_{\alpha_1}(u_m^0) + a_{ijh1}(\xi)\frac{\partial N_{\alpha_1 hm}(\xi)}{\partial \xi}\Psi_j \Psi_{\alpha_1}(u_m^0) \\
&\quad + a_{ijhk}(\xi)\Psi_j \Psi_k(u_h^0) - \hat{a}_{ijhk}\Psi_j \Psi_k(u_h^0)
\end{aligned} \tag{28}$$

Let $\mathbf{N}_{\alpha_1\alpha_2}(\xi)$ is the solution of the following problem:

$$\begin{cases}
\frac{\partial}{\partial \xi}\left(a_{i1h1}(\xi)\frac{\partial N_{\alpha_1\alpha_2 hm}(\xi)}{\partial \xi}\right) = \hat{a}_{i\alpha_1 m\alpha_2} - a_{i\alpha_1 m\alpha_2} \\
\qquad - a_{i\alpha_1 h1}(\xi)\frac{\partial N_{\alpha_2 hm}(\xi)}{\partial \xi} - \frac{\partial}{\partial \xi}\left(a_{i1h\alpha_1}(\xi)N_{\alpha_2 hm}(\xi)\right) & \xi \in Q_r \\
N_{\alpha_1\alpha_2 m}(\xi) = 0 & \xi \in \partial Q_r
\end{cases} \tag{29}$$

where $\mathbf{N}_{\alpha_1\alpha_2}(\xi)$ $(\alpha_1,\alpha_2 = 1,2,3,4)$ are matrix valued functions. It has the following forms

$$\mathbf{N}_{\alpha_1\alpha_2}(\xi) = \begin{pmatrix} N_{\alpha_1\alpha_2 11}(\xi) & N_{\alpha_1\alpha_2 12}(\xi) & N_{\alpha_1\alpha_2 13}(\xi) \\ N_{\alpha_1\alpha_2 21}(\xi) & N_{\alpha_1\alpha_2 22}(\xi) & N_{\alpha_1\alpha_2 23}(\xi) \\ N_{\alpha_1\alpha_2 31}(\xi) & N_{\alpha_1\alpha_2 32}(\xi) & N_{\alpha_1\alpha_2 33}(\xi) \end{pmatrix}$$

Similar to (23), it is easy to prove that (29) also has the unique solution $\mathbf{N}_{\alpha_1\alpha_2 m}(\xi)$. Substitute (29) into (28), then

$$\frac{\partial}{\partial \xi}\left[a_{i1h1}(\xi)\frac{\partial}{\partial \xi}\left(u_{2,h}(r,\xi,\theta,z) - N_{\alpha_1\alpha_2 hm}(\xi)\Psi_{\alpha_1}\Psi_{\alpha_2}(u_m^0)\right)\right] = 0 \tag{30}$$

The equation (30) has a specific solution with the following forms

$$\mathbf{u}_2(r,\xi,\theta,z) = \mathbf{N}_{\alpha_1\alpha_2}(\xi)\Psi_{\alpha_1}\Psi_{\alpha_2}\left(\mathbf{u}^0(r,\theta,z)\right) \tag{31}$$

Summing up, one acquires the following theorem.

Theorem 3.1. *The mechanical problem* (9) *of LCCS has the formally approximate solution as follows*:

$$\mathbf{u}^\varepsilon(r,\theta,z) \cong \mathbf{u}^0(r,\theta,z) + \varepsilon\mathbf{N}_{\alpha_1}(\xi)\Psi_{\alpha_1}\left(\mathbf{u}^0(r,\theta,z)\right) + \varepsilon^2\mathbf{N}_{\alpha_1\alpha_2}(\xi)\Psi_{\alpha_1}\Psi_{\alpha_2}\left(\mathbf{u}^0(r,\theta,z)\right) \tag{32}$$

where $\Psi_{\alpha_1}, \Psi_{\alpha_2}, (\alpha_1, \alpha_2 = 1,2,3,4)$ *are differential operators and* $\Psi_1 = \frac{\partial}{\partial r}$, $\Psi_2 = \frac{1}{r}\frac{\partial}{\partial\theta}, \Psi_3 = \frac{\partial}{\partial z}, \Psi_4 = \frac{1}{r}$, and $\mathbf{u}^0(r,\theta,z)$ *is the solution of the homogenized problem* (10), *called as the homogenization solution*, $\mathbf{N}_{\alpha_1}(\xi)$ *and* $\mathbf{N}_{\alpha_1\alpha_2}(\xi)$ *are the solutions of the problems* (23) *and* (29), *respectively*.

Remark 3.2. From (10), the homogenized equation of plane axis-symmetric problem without body force is reduced to

$$\hat{a}_{1111}\frac{\partial^2 u_r^0}{\partial r^2} + (\hat{a}_{1411} + \hat{a}_{1114})\frac{1}{r}\frac{\partial u_r^0}{\partial r} + (\hat{a}_{1414} - \hat{a}_{1114})\frac{u_r^0}{r^2} = 0 \tag{33}$$

Suppose that the material is isotropic in each lamina of LCCS. Then from the Green's formula and the equation (23), one obtains

$$\begin{cases} \hat{a}_{1111} = \hat{a}_{1411} + \hat{a}_{1114} \\ \hat{a}_{1414} - \hat{a}_{1114} = -\hat{a}_{1111} + \dfrac{1}{|Q_r|}\displaystyle\int_{Q_r} a_{1411}(\xi)\frac{\partial}{\partial\xi}\left(N_{111}(\xi) + N_{411}(\xi)\right)d\xi \end{cases} \tag{34}$$

Let $\bar{c}_{11} = \hat{a}_{1111} = \hat{a}_{1411} + \hat{a}_{1114}$ and $\bar{c}_{22} = \hat{a}_{1414} - \hat{a}_{1114}$, then usually $\bar{c}_{11} \neq \bar{c}_{22}$. In other words, although the material is isotropic in each lamina, the homogenized parameters of LCCS don't show isotropy under cylindrical coordinate system. Then the equation (33) is rewritten as

$$\bar{c}_{11}\frac{\partial^2 u_r^0}{\partial r^2} + \bar{c}_{11}\frac{1}{r}\frac{\partial u_r^0}{\partial r} - \bar{c}_{22}\frac{u_r^0}{r^2} = 0 \tag{35}$$

4. Formulation for strains and stresses of two typical problems

4.1 Plane axis-symmetric problem of cylinder with uniform pressure

Considering the LCCS subject to the uniform inner and outer pressures, shown in Fig.2, the following loading condition is given

$$\begin{cases} r = a: \quad \sigma_r = -p_a; \quad \tau_{r\theta} = 0 \\ r = b: \quad \sigma_r = -p_b; \quad \tau_{r\theta} = 0 \end{cases} \tag{36}$$

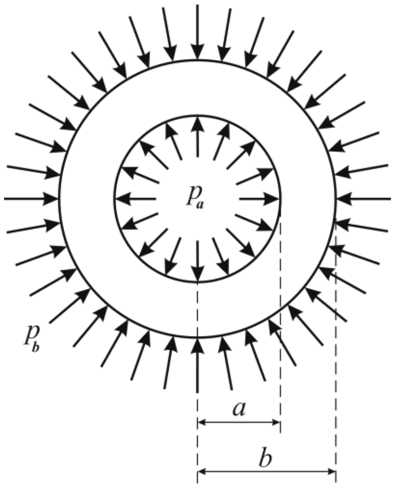

Fig. 2. A cylindrical structure subject to inner and outer pressures

The balance equation (35) without body force is obtained from remark 3.2. There exists the following solution from elasticity mechanics

$$u_r^0 = \frac{1}{\bar{c}_{12} + k\bar{c}_{11}} \cdot \frac{1}{b^{2k} - a^{2k}} \left(a^{k+1} p_a - b^{k+1} p_b\right) r^k + \frac{1}{\bar{c}_{12} - k\bar{c}_{11}} \cdot \frac{a^{k+1} b^{k+1}}{b^{2k} - a^{2k}} \left(a^{k-1} p_b - b^{k-1} p_a\right) \frac{1}{r^k} \tag{37}$$

where $k = \sqrt{\frac{\bar{c}_{22}}{\bar{c}_{11}}}$, the homogenized elasticity coefficient of torus is $\bar{\mathrm{C}} = \begin{bmatrix} \bar{c}_{11} & \bar{c}_{12} \\ \bar{c}_{21} & \bar{c}_{22} \end{bmatrix}$.

From (32), the displacement u_r^{ε} has the formally second-order approximate expression as follows

$$u_r^{\varepsilon,2}(r) = u_r^0(r) + \varepsilon N_{\alpha_1 11}(\xi) \Psi_{\alpha_1}\left(u_r^0(r)\right) + \varepsilon^2 N_{\alpha_1\alpha_2 11}(\xi) \Psi_{\alpha_1} \Psi_{\alpha_2}\left(u_r^0(r)\right) \tag{38}$$

where $\mathbf{N}_{\alpha_1}(\xi)$ and $\mathbf{N}_{\alpha_1\alpha_2}(\xi)$ are the solutions of the problems (23) and (29), respectively.

In order to unify the symbol in this paper, let $\Psi_{\alpha_1}, \Psi_{\alpha_2}, \left(\alpha_1, \alpha_2 = 1,4\right)$, $\Psi_1 = \frac{\partial}{\partial r}, \Psi_4 = \frac{1}{r}$.

Substituting (38) into Geometry Equation one obtains the following strain expressions

$$
\begin{cases}
\varepsilon_r(r) = \dfrac{\partial u_r^{\varepsilon,2}(r)}{\partial r} = \dfrac{\partial u_r^0(r)}{\partial r} + \dfrac{\partial N_{\alpha_1 11}(\xi)}{\partial \xi}\Psi_{\alpha_1}\left(u_r^0(r)\right) + \varepsilon N_{\alpha_1 11}(\xi)\Psi_1\left(\Psi_{\alpha_1}\left(u_r^0(r)\right)\right) \\
\qquad + \varepsilon \dfrac{\partial N_{\alpha_1\alpha_2 11}(\xi)}{\partial \xi}\Psi_{\alpha_1}\Psi_{\alpha_2}\left(u_r^0(r)\right) + \varepsilon^2 N_{\alpha_1\alpha_2 11}(\xi)\Psi_1\left(\Psi_{\alpha_1}\Psi_{\alpha_2}\left(u_r^0(r)\right)\right) \\
\varepsilon_\theta(r) = \dfrac{u_r^{\varepsilon,2}(r)}{r} = \dfrac{u_r^0(r)}{r} + \varepsilon \dfrac{1}{r} N_{\alpha_1 11}(\xi)\Psi_{\alpha_1}\left(u_r^0(r)\right) + \varepsilon^2 \dfrac{1}{r} N_{\alpha_1\alpha_2 11}(\xi)\Psi_{\alpha_1}\Psi_{\alpha_2}\left(u_r^0(r)\right)
\end{cases}
\tag{39}
$$

The elasticity coefficient satisfies $c_{ij}^{\varepsilon}(r) = c_{ij}(\xi)$ according to (11) and (8). Based on Hooke's law, the stresses are evaluated

$$
\begin{cases}
\sigma_r(r) = c_{11}(\xi)\dfrac{\partial u_r^0(r)}{\partial r} + c_{11}(\xi)\dfrac{\partial N_{\alpha_1 11}(\xi)}{\partial \xi}\Psi_{\alpha_1}\left(u_r^0(r)\right) + \varepsilon c_{11}(\xi) N_{\alpha_1 11}(\xi)\Psi_1\left(\Psi_{\alpha_1}\left(u_r^0(r)\right)\right) \\
\qquad + \varepsilon c_{11}(\xi)\dfrac{\partial N_{\alpha_1\alpha_2 11}(\xi)}{\partial \xi}\Psi_{\alpha_1}\Psi_{\alpha_2}\left(u_r^0(r)\right) + \varepsilon^2 c_{11}(\xi) N_{\alpha_1\alpha_2 11}(\xi)\Psi_1\left(\Psi_{\alpha_1}\Psi_{\alpha_2}\left(u_r^0(r)\right)\right) \\
\qquad + c_{12}(\xi)\dfrac{u_r^0(r)}{r} + \varepsilon c_{12}(\xi)\dfrac{1}{r} N_{\alpha_1 11}(\xi)\Psi_{\alpha_1}\left(u_r^0(r)\right) \\
\qquad + \varepsilon^2 c_{12}(\xi)\dfrac{1}{r} N_{\alpha_1\alpha_2 11}(\xi)\Psi_{\alpha_1}\Psi_{\alpha_2}\left(u_r^0(r)\right) \\
\sigma_\theta(r) = c_{21}(\xi)\dfrac{\partial u_r^0(r)}{\partial r} + c_{21}(\xi)\dfrac{\partial N_{\alpha_1 11}(\xi)}{\partial \xi}\Psi_{\alpha_1}\left(u_r^0(r)\right) + \varepsilon c_{21}(\xi) N_{\alpha_1 11}(\xi)\Psi_1\left(\Psi_{\alpha_1}\left(u_r^0(r)\right)\right) \\
\qquad + \varepsilon c_{21}(\xi)\dfrac{\partial N_{\alpha_1\alpha_2 11}(\xi)}{\partial \xi}\Psi_{\alpha_1}\Psi_{\alpha_2}\left(u_r^0(r)\right) + \varepsilon^2 c_{21}(\xi) N_{\alpha_1\alpha_2 11}(\xi)\Psi_1\left(\Psi_{\alpha_1}\Psi_{\alpha_2}\left(u_r^0(r)\right)\right) \\
\qquad + c_{22}(\xi)\dfrac{u_r^0(r)}{r} + \varepsilon c_{22}(\xi)\dfrac{1}{r} N_{\alpha_1 11}(\xi)\Psi_{\alpha_1}\left(u_r^0(r)\right) \\
\qquad + \varepsilon^2 c_{22}(\xi)\dfrac{1}{r} N_{\alpha_1\alpha_2 11}(\xi)\Psi_{\alpha_1}\Psi_{\alpha_2}\left(u_r^0(r)\right)
\end{cases}
\tag{40}
$$

Substituting (37) and operators $\Psi_1 = \dfrac{\partial}{\partial r}, \Psi_4 = \dfrac{1}{r}$ into (39), the strain expressions are rewritten as follows in detail

$$
\begin{cases}
\varepsilon_r(r) = \left[k\left(1+\frac{\partial N_{111}(\xi)}{\partial \xi}\right)+\frac{\partial N_{411}(\xi)}{\partial \xi}\right]Ar^{k-1}+\left[\frac{\partial N_{411}(\xi)}{\partial \xi}-k\left(1+\frac{\partial N_{111}(\xi)}{\partial \xi}\right)\right]\frac{B}{r^{k+1}} \\
\quad +\varepsilon\left[k(k-1)\left(N_{111}(\xi)+\frac{\partial N_{1111}(\xi)}{\partial \xi}\right)+(k-1)\left(N_{411}(\xi)+\frac{\partial N_{1411}(\xi)}{\partial \xi}\right)\right. \\
\quad\quad \left. +k\frac{\partial N_{4111}(\xi)}{\partial \xi}+\frac{\partial N_{4411}(\xi)}{\partial \xi}\right]Ar^{k-2} \\
\quad +\varepsilon\left[k(k+1)\left(N_{111}(\xi)+\frac{\partial N_{1111}(\xi)}{\partial \xi}\right)-(k+1)\left(N_{411}(\xi)+\frac{\partial N_{1411}(\xi)}{\partial \xi}\right)\right. \\
\quad\quad \left. -k\frac{\partial N_{4111}(\xi)}{\partial \xi}+\frac{\partial N_{4411}(\xi)}{\partial \xi}\right]\frac{B}{r^{k+2}} \\
\quad +\varepsilon^2\left[k(k-1)(k-2)N_{1111}(\xi)+(k-1)(k-2)N_{1411}(\xi)\right. \\
\quad\quad \left. +k(k-2)N_{4111}(\xi)+(k-2)N_{4411}(\xi)\right]Ar^{k-3} \\
\quad -\varepsilon^2\left[k(k+1)(k+2)N_{1111}(\xi)-(k+1)(k+2)N_{1411}(\xi)\right. \\
\quad\quad \left. -k(k+2)N_{4111}(\xi)+(k+2)N_{4411}(\xi)\right]\frac{B}{r^{k+3}} \\
\varepsilon_\theta(r) = \left(Ar^{k-1}+\frac{B}{r^{k+1}}\right)+\varepsilon\left(kN_{111}(\xi)+N_{411}(\xi)\right)Ar^{k-2}-\varepsilon\left(kN_{111}(\xi)-N_{411}(\xi)\right)\frac{B}{r^{k+2}} \\
\quad +\varepsilon^2\left[k(k-1)N_{1111}(\xi)+(k-1)N_{1411}(\xi)+kN_{4111}(\xi)+N_{4411}(\xi)\right]Ar^{k-3} \\
\quad +\varepsilon^2\left[k(k+1)N_{1111}(\xi)-(k+1)N_{1411}(\xi)-kN_{4111}(\xi)+N_{4411}(\xi)\right]\frac{B}{r^{k+3}}
\end{cases} \tag{41}
$$

where $\begin{cases} k=\sqrt{\dfrac{\bar{c}_{22}}{\bar{c}_{11}}} \\ A=\dfrac{1}{\bar{c}_{12}+k\bar{c}_{11}}\cdot\dfrac{1}{b^{2k}-a^{2k}}\left(a^{k+1}p_a-b^{k+1}p_b\right) \\ B=\dfrac{1}{\bar{c}_{12}-k\bar{c}_{11}}\cdot\dfrac{a^{k+1}b^{k+1}}{b^{2k}-a^{2k}}\left(a^{k-1}p_b-b^{k-1}p_a\right) \end{cases}$ and $\xi=\dfrac{r-r_0}{\varepsilon}$.

Furthermore, by the above strains expressions (41) and Hooke's law, the stresses can be evaluated anywhere in global cross section of structure. Then based on the first-ply failure criterion, the elastic limit load of LCCS can be evaluated.

4.2 Spatially axis-symmetric problem of cylinder with linearly varying pressures

A LCCS bears linearly varying inner and outer pressures as shown in Fig.3, where the inner and outer radiuses of cylinder are a and b, respectively. And p_a, p_b are the inner and outer pressures at $z=0$. $p_a^*/l, p_b^*/l$ are slopes of the inner and outer pressure variation, respectively. And the boundary conditions are satisfied

$$r=\mathrm{a}, \begin{cases} \sigma_r = p_a^*\left(\dfrac{z}{l}\right) + p_a; \\ \tau_{rz} = 0 \end{cases} \quad r=b, \begin{cases} \sigma_r = p_b^*\left(\dfrac{z}{l}\right) + p_b; \\ \tau_{rz} = 0 \end{cases} \quad z=0 \text{ or } l, \begin{cases} \sigma_z = 0 \\ \tau_{rz} = 0 \end{cases} \tag{42}$$

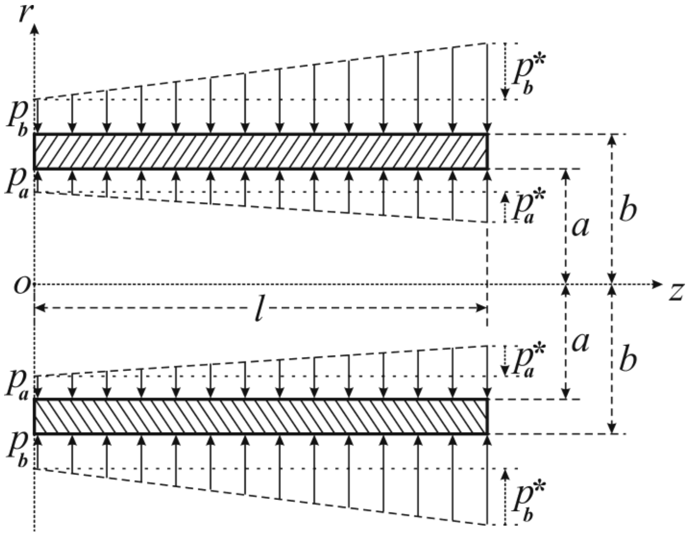

Fig. 3. The $r-z$ section of cylinder subject to linearly varying inner and outer pressures

From [8, 9], the stress solutions of cylinder made by isotropic materials are found

$$\begin{cases} \sigma_r = \dfrac{z}{l}\cdot\dfrac{a^2b^2}{b^2-a^2}\left[p_b^*\left(\dfrac{1}{a^2}-\dfrac{1}{r^2}\right)+p_a^*\left(\dfrac{1}{r^2}-\dfrac{1}{b^2}\right)\right] \\ \qquad +\dfrac{a^2b^2}{b^2-a^2}\left[p_b\left(\dfrac{1}{a^2}-\dfrac{1}{r^2}\right)+p_a\left(\dfrac{1}{r^2}-\dfrac{1}{b^2}\right)\right] \\ \sigma_\theta = \dfrac{z}{l}\cdot\dfrac{a^2b^2}{b^2-a^2}\left[p_b^*\left(\dfrac{1}{a^2}+\dfrac{1}{r^2}\right)-p_a^*\left(\dfrac{1}{r^2}+\dfrac{1}{b^2}\right)\right] \\ \qquad +\dfrac{a^2b^2}{b^2-a^2}\left[p_b\left(\dfrac{1}{a^2}+\dfrac{1}{r^2}\right)-p_a\left(\dfrac{1}{r^2}+\dfrac{1}{b^2}\right)\right] \\ \sigma_z = 0 \\ \tau_{rz} = \tau_{zr} = 0 \end{cases} \tag{43}$$

Using constitutive equation (3) and geometry equation (2), the following homogenization displacements are gotten

$$
\begin{cases}
u_r = \dfrac{1-\nu}{E}\dfrac{p_b^* b^2 - p_a^* a^2}{l(b^2-a^2)}\cdot z\cdot r + \dfrac{1+\nu}{E}\dfrac{a^2b^2(p_b^*-p_a^*)}{l(b^2-a^2)}\cdot\dfrac{z}{r} \\
\qquad + \dfrac{1-\nu}{E}\dfrac{p_b b^2 - p_a a^2}{b^2-a^2}\cdot r + \dfrac{1+\nu}{E}\dfrac{a^2b^2(p_b-p_a)}{b^2-a^2}\cdot\dfrac{1}{r} \\
u_z = -\dfrac{\nu}{E}\dfrac{p_b^* b^2 - p_a^* a^2}{l(b^2-a^2)}\cdot z^2 - \dfrac{2\nu}{E}\dfrac{p_b b^2 - p_a a^2}{b^2-a^2} z \\
\qquad - \dfrac{1-\nu}{E}\dfrac{p_b^* b^2 - p_a^* a^2}{l(b^2-a^2)}\cdot\dfrac{1}{2} r^2 - \dfrac{1+\nu}{E}\dfrac{a^2b^2(p_b^*-p_a^*)}{l(b^2-a^2)}\cdot \ln r + C
\end{cases}
\tag{44}
$$

where E is the Young's modulus, ν is the Poisson ratio, and C is a constant.

In terms of (32), the displacement u_r^{ε} has the formally second-order approximate expression as follows

$$
u_h^{\varepsilon,2} = u_h^0 + \varepsilon N_{\alpha_1 hm}(\xi)\Psi_{\alpha_1}(u_m^0) + \varepsilon^2 N_{\alpha_1\alpha_2 hm}(\xi)\Psi_{\alpha_1}\Psi_{\alpha_2}(u_m^0)
\tag{45}
$$

Substituting (45) into geometry equation (2), we have the strain expressions

$$
\begin{cases}
\varepsilon_r(r,z) = \dfrac{\partial u_r^0(r,z)}{\partial r} + \dfrac{\partial N_{\alpha_1 1m}(\xi)}{\partial \xi}\Psi_{\alpha_1}\left(u_m^0(r,z)\right) + \varepsilon N_{\alpha_1 1m}(\xi)\Psi_1\left(\Psi_{\alpha_1}\left(u_m^0(r,z)\right)\right) \\
\qquad + \varepsilon\dfrac{\partial N_{\alpha_1\alpha_2 1m}(\xi)}{\partial \xi}\Psi_{\alpha_1}\Psi_{\alpha_2}\left(u_m^0(r,z)\right) + \varepsilon^2 N_{\alpha_1\alpha_2 1m}(\xi)\Psi_1\left(\Psi_{\alpha_1}\Psi_{\alpha_2}\left(u_m^0(r,z)\right)\right) \\
\varepsilon_\theta(r,z) = \dfrac{u_r^0(r,z)}{r} + \varepsilon N_{\alpha_1 1m}(\xi)\dfrac{1}{r}\Psi_{\alpha_1}\left(u_m^0(r,z)\right) + \varepsilon^2 N_{\alpha_1\alpha_2 1m}(\xi)\dfrac{1}{r}\Psi_{\alpha_1}\Psi_{\alpha_2}\left(u_m^0(r,z)\right) \\
\varepsilon_z(r,z) = \dfrac{\partial u_z^0(r,z)}{\partial z} + \varepsilon N_{\alpha_1 3m}(\xi)\Psi_3\left(\Psi_{\alpha_1}\left(u_m^0(r,z)\right)\right) + \varepsilon^2 N_{\alpha_1\alpha_2 3m}(\xi)\Psi_3\left(\Psi_{\alpha_1}\Psi_{\alpha_2}\left(u_m^0(r,z)\right)\right) \\
\gamma_{zr}(r,z) = \dfrac{\partial u_z^0(r,z)}{\partial r} + \dfrac{\partial N_{\alpha_1 3m}(\xi)}{\partial \xi}\Psi_{\alpha_1}\left(u_m^0(r,z)\right) + \varepsilon N_{\alpha_1 3m}(\xi)\Psi_1\left(\Psi_{\alpha_1}\left(u_m^0(r,z)\right)\right) \\
\qquad + \varepsilon\dfrac{\partial N_{\alpha_1\alpha_2 3m}(\xi)}{\partial \xi}\Psi_{\alpha_1}\Psi_{\alpha_2}\left(u_m^0(r,z)\right) + \varepsilon^2 N_{\alpha_1\alpha_2 3m}(\xi)\Psi_1\left(\Psi_{\alpha_1}\Psi_{\alpha_2}\left(u_m^0(r,z)\right)\right) \\
\qquad + \dfrac{\partial u_r^0(r,z)}{\partial z} + \varepsilon N_{\alpha_1 1m}(\xi)\Psi_3\left(\Psi_{\alpha_1}\left(u_m^0(r,z)\right)\right) + \varepsilon^2 N_{\alpha_1\alpha_2 1m}(\xi)\Psi_3\left(\Psi_{\alpha_1}\Psi_{\alpha_2}\left(u_m^0(r,z)\right)\right)
\end{cases}
\tag{46}
$$

Then the stress expressions can be also evaluated based on the expressions (46) and Hooke's law.

Moreover, one finds $a_{ij34} = 0$; $a_{ij13} = a_{ij31}$, $i = 1,2,3$, $j = 1,2,3,4$ from (8) and obtains $N_{4h3} = 0$, $N_{\alpha_1 4h3} = 0$; $N_{1h3} = N_{3h1}$, $N_{\alpha_1 1h3} = N_{\alpha_1 3h1}$, $h = 1,2,3$, $\alpha_1 = 1,2,3,4$ from (23) and (29). At the same time, one obtains $\dfrac{\partial^k u_r}{\partial z^k} = 0, \forall k \geq 2$, $\dfrac{\partial^l u_z}{\partial z^l} = 0, \ \forall l \geq 3$,

$\frac{\partial^{m+n} u_z}{\partial r^m \partial z^n} = 0, \forall m \geq 1, n \geq 1$ from (44). And then inserting the homogenization displacement (44) and the operators $\Psi_1 = \frac{\partial}{\partial r}, \Psi_3 = \frac{\partial}{\partial z}, \Psi_4 = \frac{1}{r}$ into (46), the detailed strain expressions are obtained

$$
\begin{aligned}
\varepsilon_r(r,z) = &\left[\left(1 + \frac{\partial N_{111}(\xi)}{\partial \xi} + \frac{\partial N_{411}(\xi)}{\partial \xi}\right)\frac{1-\nu}{E} - 2\frac{\partial N_{313}(\xi)}{\partial \xi}\frac{\nu}{E}\right]\left(A^* z + A\right) \\
&- \left(1 + \frac{\partial N_{111}(\xi)}{\partial \xi} - \frac{\partial N_{411}(\xi)}{\partial \xi}\right)\frac{1+\nu}{E}\frac{(B^* z + B)}{r^2} \\
&+ \varepsilon\left[\left(\frac{\partial N_{3111}(\xi)}{\partial \xi} + \frac{\partial N_{3411}(\xi)}{\partial \xi}\right)\frac{1-\nu}{E} - 2\frac{\partial N_{3313}(\xi)}{\partial \xi}\frac{\nu}{E}\right]A^* \\
&+ \varepsilon\left(\left(\frac{\partial N_{4111}(\xi)}{\partial \xi} + \frac{\partial N_{4411}(\xi)}{\partial \xi}\right)\frac{1-\nu}{E} - 2\frac{\partial N_{4313}(\xi)}{\partial \xi}\frac{\nu}{E}\right)\frac{(A^* z + A)}{r} \\
&+ \varepsilon\left(2N_{111}(\xi) + 2\frac{\partial N_{1111}(\xi)}{\partial \xi} - 2N_{411}(\xi) - 2\frac{\partial N_{1411}(\xi)}{\partial \xi}\right. \\
&\qquad \left. - \frac{\partial N_{4111}(\xi)}{\partial \xi} + \frac{\partial N_{4411}(\xi)}{\partial \xi}\right)\frac{1+\nu}{E}\frac{(B^* z + B)}{r^3} \\
&+ \varepsilon\left(\frac{\partial N_{3411}(\xi)}{\partial \xi} - \frac{\partial N_{3111}(\xi)}{\partial \xi}\right)\frac{1+\nu}{E}\frac{B^*}{r^2} \\
&+ \varepsilon^2\left(2N_{4313}(\xi)\frac{\nu}{E} - \left(N_{4111}(\xi) + N_{4411}(\xi)\right)\frac{1-\nu}{E}\right)\frac{(A^* z + A)}{r^2} \\
&+ \varepsilon^2\left(6N_{1411}(\xi) - 6N_{1111}(\xi) + 3N_{4111}(\xi) - 3N_{4411}(\xi)\right)\frac{1+\nu}{E}\frac{(B^* z + B)}{r^4} \\
&+ \varepsilon^2\left(2N_{3111}(\xi) - 2N_{3411}(\xi)\right)\frac{1+\nu}{E}\frac{B^*}{r^3}
\end{aligned} \tag{47}
$$

$$
\begin{aligned}
\varepsilon_\theta(r,z) = {} & \frac{1-\nu}{E}(A^*z+A) + \frac{1+\nu}{E}\frac{(B^*z+B)}{r^2} \\
& + \varepsilon\left(\left(N_{111}(\xi) + N_{411}(\xi)\right)\frac{1-\nu}{E} - 2N_{313}(\xi)\frac{\nu}{E} \right)\frac{(A^*z+A)}{r} \\
& + \varepsilon\left(N_{411}(\xi) - N_{111}(\xi)\right)\frac{1+\nu}{E}\frac{(B^*z+B)}{r^3} \\
& + \varepsilon^2\left(\left(N_{4111}(\xi) + N_{4411}(\xi)\right)\frac{1-\nu}{E} - 2N_{4313}(\xi)\frac{\nu}{E} \right)\frac{(A^*z+A)}{r^2} \\
& + \varepsilon^2\left(2N_{1111}(\xi) - 2N_{1411}(\xi) + N_{4411}(\xi) - N_{4111}(\xi)\right)\frac{1+\nu}{E}\frac{(B^*z+B)}{r^4} \\
& + \varepsilon^2\left(\left(N_{3111}(\xi) + N_{3411}(\xi)\right)\frac{1-\nu}{E} - 2N_{3313}(\xi)\frac{\nu}{E} \right)\frac{A^*}{r} \\
& + \varepsilon^2\left(N_{3411}(\xi) - N_{3111}(\xi)\right)\frac{1+\nu}{E}\frac{B^*}{r^3}
\end{aligned} \tag{48}
$$

$$
\begin{aligned}
\varepsilon_z(r,z) = {} & -\frac{\nu}{E}\left(A^*z+A\right) \\
& + \varepsilon\left(\left(N_{131}(\xi) + N_{431}(\xi)\right)\frac{1-\nu}{E} - 2N_{333}(\xi)\frac{\nu}{E} \right)A^* \\
& + \varepsilon\left(N_{431}(\xi) - N_{131}(\xi)\right)\frac{1+\nu}{E}\frac{B^*}{r^2} \\
& + \varepsilon^2\left(\left(N_{4131}(\xi) + N_{4431}(\xi)\right)\frac{1-\nu}{E} - 2N_{4333}(\xi)\frac{\nu}{E} \right)\frac{A^*}{r} \\
& + \varepsilon^2\left(2N_{1131}(\xi) + N_{4431}(\xi) - 2N_{1431}(\xi) - N_{4131}(\xi)\right)\frac{1+\nu}{E}\frac{B^*}{r^3}
\end{aligned} \tag{49}
$$

$$
\begin{aligned}
\gamma_{zr}(r,z) = & \left[\left(\frac{\partial N_{131}(\xi)}{\partial \xi}+\frac{\partial N_{431}(\xi)}{\partial \xi}\right)\frac{1-\nu}{E}-2\frac{\partial N_{333}(\xi)}{\partial \xi}\frac{\nu}{E}\right](A^{*}z+A) \\
& +\left(\frac{\partial N_{431}(\xi)}{\partial \xi}-\frac{\partial N_{131}(\xi)}{\partial \xi}\right)\frac{1+\nu}{E}\frac{(B^{*}z+B)}{r^{2}} \\
& +\varepsilon\left[\left(N_{111}(\xi)+N_{411}(\xi)+\frac{\partial N_{3131}(\xi)}{\partial \xi}+\frac{\partial N_{3431}(\xi)}{\partial \xi}\right)\frac{1-\nu}{E}\right. \\
& \quad \left. -2\left(N_{313}(\xi)+\frac{\partial N_{3333}(\xi)}{\partial \xi}\right)\frac{\nu}{E}\right]A^{*} \\
& +\varepsilon\left[\left(\frac{\partial N_{4131}(\xi)}{\partial \xi}+\frac{\partial N_{4431}(\xi)}{\partial \xi}\right)\frac{1-\nu}{E}-2\frac{\partial N_{4333}(\xi)}{\partial \xi}\frac{\nu}{E}\right]\frac{(A^{*}z+A)}{r} \\
& +\varepsilon\left(2N_{131}(\xi)+2\frac{\partial N_{1131}(\xi)}{\partial \xi}-2N_{431}(\xi)-2\frac{\partial N_{1431}(\xi)}{\partial \xi}\right. \\
& \quad \left. -\frac{\partial N_{4131}(\xi)}{\partial \xi}+\frac{\partial N_{4431}(\xi)}{\partial \xi}\right)\frac{1+\nu}{E}\frac{(B^{*}z+B)}{r^{3}} \\
& +\varepsilon\left(N_{411}(\xi)-N_{111}(\xi)+\frac{\partial N_{3431}(\xi)}{\partial \xi}-\frac{\partial N_{3131}(\xi)}{\partial \xi}\right)\frac{1+\nu}{E}\frac{B^{*}}{r^{2}} \\
& +\varepsilon^{2}\left(2N_{4333}(\xi)\frac{\nu}{E}-\left(N_{4131}(\xi)+N_{4431}(\xi)\right)\frac{1-\nu}{E}\right)\frac{(A^{*}z+A)}{r^{2}} \\
& +\varepsilon^{2}\left(-6N_{1131}(\xi)+6N_{1431}(\xi)+3N_{4131}(\xi)-3N_{4431}(\xi)\right)\frac{1+\nu}{E}\frac{(B^{*}z+B)}{r^{4}} \\
& +\varepsilon^{2}\left(\left(N_{4411}(\xi)+N_{4111}(\xi)\right)\frac{1-\nu}{E}-2N_{4313}(\xi)\frac{\nu}{E}\right)\frac{A^{*}}{r} \\
& +\varepsilon^{2}\left(2N_{3131}(\xi)-2N_{3431}(\xi)+2N_{1111}(\xi)-2N_{1411}(\xi)\right. \\
& \quad \left. -N_{4111}(\xi)+N_{4411}(\xi)\right)\frac{1+\nu}{E}\frac{B^{*}}{r^{3}}
\end{aligned} \tag{50}
$$

where $\begin{cases} A^{*}=\dfrac{p_b^{*}b^{2}-p_a^{*}a^{2}}{l(b^{2}-a^{2})} \ ; \ B^{*}=\dfrac{a^{2}b^{2}(p_b^{*}-p_a^{*})}{l(b^{2}-a^{2})} \\ A=\dfrac{p_b b^{2}-p_a a^{2}}{b^{2}-a^{2}} \ ; \ B=\dfrac{a^{2}b^{2}(p_b-p_a)}{b^{2}-a^{2}} \end{cases}$ and $\xi=\dfrac{r-r_0}{\varepsilon}$.

Making use of the stress-strain relation, one can evaluate the stresses anywhere inside the cylinder. And then according to the yield criterion, the elasticity critical load of cylinder subject to linearly varying pressure can be evaluated. It is worthy of note, if the homogenized stiffness parameters are not isotropic, the solutions (43) and (44) don’t hold, herewith, each formula of (46)-(50) is unsuitable.

Similarly, one can obtain the expressions of strain and stress for LCCS subject to other loads and constrains.

5 Finite element computation of the second-order and two-scale method in cylindrical coordinates

5.1 FE approximate formulas

1. **FE solutions for $\mathbf{N}_{\alpha_1 m}(\xi)$ and the approximate stiffness coefficients** $\{\hat{a}_{ijhk}^h\}$.

   From (26) the approximate elasticity stiffness coefficients $\{\hat{a}_{ijhk}^h\}$ are calculated after the approximate solutions $\mathbf{N}_{\alpha_1 m}^h(\xi)$ of problem (23) are obtained.

From the variational principles it follows that the problem (23) is equivalent to the following virtual work equation

$$\int_{Q_r} \frac{\partial v_i(\xi)}{\partial \xi} a_{i1h1}(\xi) \frac{\partial N_{\alpha_1 hm}(\xi)}{\partial \xi} \mathrm{d}\xi = -\int_{Q_r} a_{i1m\alpha_1}(\xi) \frac{\partial v_i(\xi)}{\partial \xi} \mathrm{d}\xi \qquad \forall v_i \in H_0^1(Q_r) \qquad (51)$$

Thus the approximate $\mathbf{N}_{\alpha_1 m}^h(\xi)$ $(m = 1,2,3, \alpha_1 = 1,2,3,4)$ are determined by solving the following FE virtual work equation on FE space $S_0^h(Q_r) = \{\mathbf{v} \in S^h(Q_r) / \mathbf{v}(Q_r) = 0\}$

$$\sum_e \int_e \frac{\partial v_i(\xi)}{\partial \xi} a_{i1h1}(\xi) \frac{\partial N_{\alpha_1 hm}^h(\xi)}{\partial \xi} \mathrm{d}\xi = -\sum_e \int_e a_{i1m\alpha_1}(\xi) \frac{\partial v_i(\xi)}{\partial \xi} \mathrm{d}\xi \quad \forall v_i \in S_0^h(Q_r) \qquad (52)$$

Actually $\mathbf{N}_{\alpha_1 m}^h(\xi)$ are obtained by using general FE programs. Then the approximate stiffness coefficients $\{\hat{a}_{ijhk}^h\}$ are evaluated by below formula

$$\hat{a}_{ijhk}^h = \int_{Q_r} \left(a_{ijhk}(\xi) + a_{ijp1}(\xi) \frac{\partial N_{kph}^h(\xi)}{\partial \xi} \right) d\xi \qquad (53)$$

2. **FE computation of $\mathbf{N}_{\alpha_1 \alpha_2 m}(\xi)$**. The FE solutions $\mathbf{N}_{\alpha_1 \alpha_2 m}^h(\xi)$ are obtained by solving the following FE virtual work equation on unit cell Q_r corresponding to the FE meshes for $\mathbf{N}_{\alpha_1 m}^h(\xi)$.

$$\int_{Q_r} \frac{\partial v_i(\xi)}{\partial \xi} a_{i1h1}(\xi) \frac{\partial N^h_{\alpha_1\alpha_2 hm}(\xi)}{\partial \xi} \mathrm{d}\xi = -\int_{Q_r} \left[\left(\hat{a}^h_{i\alpha_1 m\alpha_2} - a_{i\alpha_1 m\alpha_2} - a_{i\alpha_1 h1}(\xi) \frac{\partial N^h_{\alpha_2 hm}(\xi)}{\partial \xi} \right) v_i(\xi) + a_{i1h\alpha_1}(\xi) N^h_{\alpha_2 hm}(\xi) \frac{\partial v_i(\xi)}{\partial \xi} \right] \mathrm{d}\xi \quad \forall v_i \in S^h_0(Q_r) \tag{54}$$

3. **Homogenization Solution**. From elasticity mechanics the homogenization solution $\mathbf{u}^0$ can be exactly obtained for typical cylindrical axis-symmetry problem or numerically evaluated by solving the FE virtual work equation corresponding to (10) on global Ω.

4. **Approximate displacement, strain and stresses**. The two-scale approximate solutions of displacement, strains and stresses anywhere on the structure Ω are evaluated by following formulas

$$u_i^{2,h}(r,\theta,z) = u_i^0(r,\theta,z) + \varepsilon N^h_{\alpha_1 im}(\xi) \Psi_{\alpha_1}\left(u^0_m(r,\theta,z)\right) + \varepsilon^2 N^h_{\alpha_1\alpha_2 im}(\xi) \Psi_{\alpha_1}\Psi_{\alpha_2}\left(u^0_m(r,\theta,z)\right) \tag{55}$$

$$\begin{cases}
\varepsilon_r^{2,h} = \dfrac{\partial u_r^0(r,\theta,z)}{\partial r} + \varepsilon N^h_{\alpha_1 1m}(\xi)\Psi_1\left(\Psi_{\alpha_1}\left(u^0_m(r,\theta,z)\right)\right) \\
\qquad + \varepsilon^2 N^h_{\alpha_1\alpha_2 1m}(\xi)\Psi_1\left(\Psi_{\alpha_1}\Psi_{\alpha_2}\left(u^0_m(r,\theta,z)\right)\right) \\
\varepsilon_\theta^{2,h} = \dfrac{1}{r}\dfrac{\partial u_\theta^0(r,\theta,z)}{\partial \theta} + \dfrac{u_r^0(r,\theta,z)}{r} + \varepsilon\left[\left(N^h_{\alpha_1 2m}(\xi)\Psi_2 + N^h_{\alpha_1 1m}(\xi)\Psi_4\right)\left(\Psi_{\alpha_1}\left(u^0_m(r,\theta,z)\right)\right)\right] \\
\qquad + \varepsilon^2\left[\left(N^h_{\alpha_1\alpha_2 2m}(\xi)\Psi_2 + N^h_{\alpha_1\alpha_2 1m}(\xi)\Psi_4\right)\left(\Psi_{\alpha_1}\Psi_{\alpha_2}\left(u^0_m(r,\theta,z)\right)\right)\right] \\
\varepsilon_z^{2,h} = \dfrac{\partial u_z^0(r,\theta,z)}{\partial z} + \varepsilon N^h_{\alpha_1 1m}(\xi)\Psi_3\left(\Psi_{\alpha_1}\left(u^0_m(r,\theta,z)\right)\right) \\
\qquad + \varepsilon^2 N^h_{\alpha_1\alpha_2 1m}(\xi)\Psi_3\left(\Psi_{\alpha_1}\Psi_{\alpha_2}\left(u^0_m(r,\theta,z)\right)\right) \\
\gamma_{r\theta}^{2,h} = \dfrac{1}{r}\dfrac{\partial u_r^0(r,\theta,z)}{\partial \theta} + \dfrac{\partial u_\theta^0(r,\theta,z)}{\partial r} - \dfrac{u_\theta^0(r,\theta,z)}{r} \\
\qquad + \varepsilon\left[\left(N^h_{\alpha_1 1m}(\xi)\Psi_2 + N^h_{\alpha_1 2m}(\xi)\Psi_1 - N^h_{\alpha_1 2m}(\xi)\Psi_4\right)\left(\Psi_{\alpha_1}\left(u^0_m(r,\theta,z)\right)\right)\right] \\
\qquad + \varepsilon^2\left[\left(N^h_{\alpha_1 1m}(\xi)\Psi_2 + N^h_{\alpha_1 2m}(\xi)\Psi_1 - N^h_{\alpha_1 2m}(\xi)\Psi_4\right)\left(\Psi_{\alpha_1}\Psi_{\alpha_2}\left(u^0_m(r,\theta,z)\right)\right)\right] \\
\gamma_{\theta z}^{2,h} = \dfrac{\partial u_\theta^0(r,\theta,z)}{\partial z} + \dfrac{1}{r}\dfrac{\partial u_z^0(r,\theta,z)}{\partial \theta} + \varepsilon\left[\left(N^h_{\alpha_1 2m}(\xi)\Psi_3 + N^h_{\alpha_1 3m}(\xi)\Psi_2\right)\left(\Psi_{\alpha_1}\left(u^0_m(r,\theta,z)\right)\right)\right] \\
\qquad + \varepsilon^2\left[\left(N^h_{\alpha_1 2m}(\xi)\Psi_3 + N^h_{\alpha_1 3m}(\xi)\Psi_2\right)\left(\Psi_{\alpha_1}\Psi_{\alpha_2}\left(u^0_m(r,\theta,z)\right)\right)\right] \\
\gamma_{zr}^{2,h} = \dfrac{\partial u_z^0(r,\theta,z)}{\partial r} + \dfrac{\partial u_r^0(r,\theta,z)}{\partial z} + \varepsilon\left[\left(N^h_{\alpha_1 3m}(\xi)\Psi_1 + N^h_{\alpha_1 1m}(\xi)\Psi_3\right)\left(\Psi_{\alpha_1}\left(u^0_m(r,\theta,z)\right)\right)\right] \\
\qquad + \varepsilon^2\left[\left(N^h_{\alpha_1 3m}(\xi)\Psi_1 + N^h_{\alpha_1 1m}(\xi)\Psi_3\right)\left(\Psi_{\alpha_1}\Psi_{\alpha_2}\left(u^0_m(r,\theta,z)\right)\right)\right]
\end{cases} \tag{56}$$

$$\sigma_i^{2,h}(r,\theta,z) = c_{ij}^{\varepsilon}(r)\varepsilon_j^{2,h}(r,\theta,z), \quad i,j = (1,2,3,4,5,6) = (r,\theta,z,r\theta,\theta z,zr) \tag{57}$$

5.2 Algorithm procedure

The algorithm procedure of the second-order and two-scale method for predicting the mechanical properties of LCCS is stated as follows

1. To determine the material parameters of each lamina in LCCS and to establish the FE model of unit cell.
2. To solve the FE virtual work equation (52) on unit cell Q_r to obtain $\mathbf{N}_{\alpha_1 m}^h(\xi)$, and then evaluate the constitutive coefficients $\{\hat{a}_{ijhk}^h\}$ by formula (53).
3. To evaluate the FE solutions $\mathbf{N}_{\alpha_1\alpha_2 m}^h(\xi)$ by solving the FE virtual work equation (54) on unit cell Q_r, using the same FE meshes in step (2) as well as the stiffness matrix and its decomposition form.
4. To obtain the homogenization displacement $\mathbf{u}^0(r,\theta,z)$ for typical problem, or numerical displacement $\mathbf{u}^{0,h}(r,\theta,z)$ for general loads and constraints by using FEM software.
5. To compute the displacements $\mathbf{u}^{2,h}(r,\theta,z)$, strains $\varepsilon_j^h(r,\theta,z)$ and stresses $\sigma_i^h(r,\theta,z)$ at arbitrary point (r,θ,z) of the structure Ω by (55), (56) and (57).
6. To evaluate the elastic limit load of LCCS according to the first-ply failure criterion.

6 Numerical experiments and results

In order to verify the feasibility and validity of the second-order and two-scale method in cylindrical coordinates for predicting mechanical properties of LCCS, we have developed the software about the STMCC, and made some numerical experiments for the mechanical parameters of LCCS. Here some numerical results are shown and compared with the results calculated by ANSYS software.

Example 1:

For the plane axis-symmetry problem of the hollow cylinders subject to uniform pressures, which is stated in Section 4.1, the stiffness parameters are computed, the elastic limit load of

LCCS is predicted and the strains and stresses are solved by STMCC. And then by analyzing the numerical results, the relation between the limit inner pressure and the size of the structure is obtained. The material of single lamina is made from carbon fiber-reinforced epoxy. The thickness of single lamina is 0.125mm and the rule of arrangement is $[45°/0°/-45°/90°]_{10}$. The global thickness of LCCS is 5mm and the inner radius is 50mm. The inner pressure is 20Mpa and the outer pressure is zero. Table 1 summarizes the stiffness and strength parameters of single composite lamina. One can obtains the equivalent stiffness properties of every lamina with different ply-angles by coordinate transformation [10, 11], shown in Table 2.

Table 1. Material properties of T300/5208 graphite-epoxy composite material

Mechanical properties	Values	Strength properties	Values
E_1 (GPa)	181	X_t (MPa)	1500.0
$E_2 = E_3$ (GPa)	10.3	X_c (MPa)	1340.0
$G_{12} = G_{13}$ (GPa)	7.17	$Y_t = Z_t$ (MPa)	57.0
$\nu_{12} = \nu_{13}$	0.28	$Y_c = Z_c$ (MPa)	212.0
ν_{23}	0.49	S (MPa)	68.0

Table 2. Mechanical parameters of cylindrical uni-directional ply with different ply angles

Fiber	Stiffness Parameters								
Orientation	E_1(GPa)	E_2(GPa)	E_3(GPa)	G_{12}(GPa)	G_{23}(GPa)	G_{13}(GPa)	ν_{12}	ν_{23}	ν_{13}
90 °	10.3	181	10.3	7.17	7.17	3.46	0.016	0.28	0.49
±45 °	12.98	25.05	25.05	4.66	46.61	4.66	0.060	0.747	0.060
0 °	10.3	10.3	181	3.46	7.17	7.17	0.49	0.016	0.016

Fig. 4 shows the variation of strain ε_r and ε_θ in radial direction, respectively. In Fig. 4(a), the smooth curve is homogenization solution of ε_r and fold line is the solution of ε_r by STMCC. The homogenization solution represents the macroscopic trend, but the second-order and two-scale solution describes the local oscillation beside the macroscopic trend, by reason that the material parameters are different in every lamina of LCCS. However, the coincidence of the homogenization solution and the second-order and two-scale solution of ε_θ is found in Fig. 4(b), which indicates that the strain in θ direction is independent of the variation of material parameters.

As a result, a relationship between the stress and the coordinate r is obtained by numerical prediction as illustrated in Fig. 5, where the smooth curve is homogenization solution and fold curve is second-order and two-scale solution. From Fig. 5(a) the numerical value of stress σ_r decreases as r increases, where the minus sign only denotes the direction of stress. And the second-order and two-scale solution of stress σ_r is oscillating with the difference of material parameters. Similarly, the circumferential stress σ_θ also has an oscillating decrease. But differently, most of the tensile stresses in circumferential direction, which are born by the laminas with 90 °ply-angles, are much larger than other stresses in the LCCS.

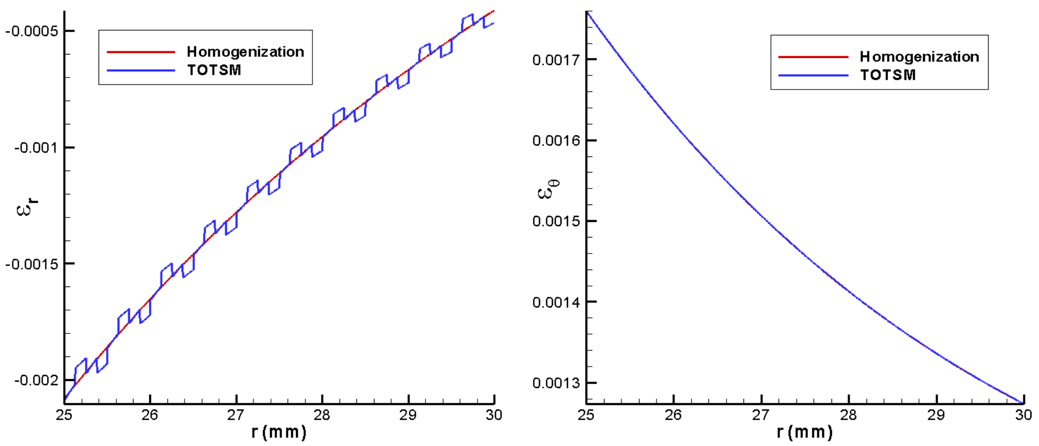

(a) ε_r in radial direction (b) ε_θ in radial direction

Fig.4. the strains of cylinder subject to uniform pressure

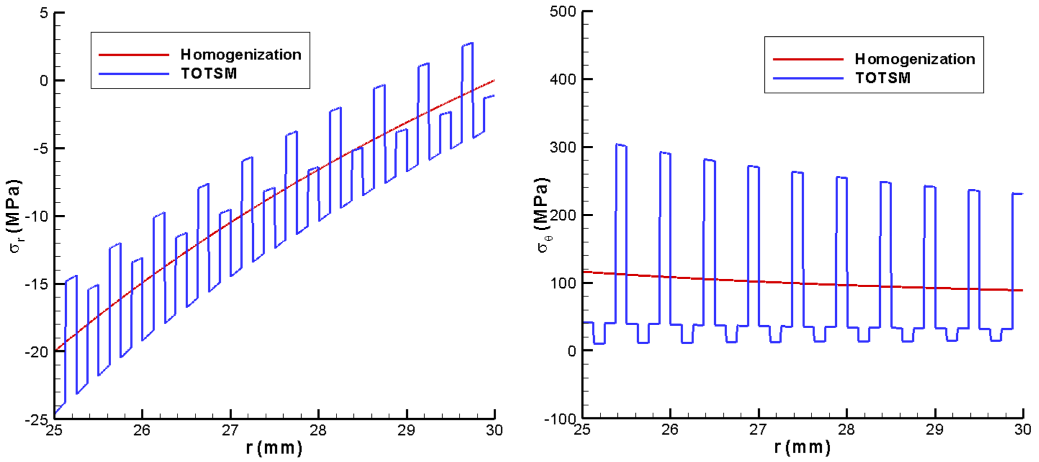

(a) σ_r in radial direction (b) σ_θ in radial direction

Fig.5. the stresses of cylinder subject to uniform pressure

Because the 90° (in circumferential direction) laminas bear the maximum stresses of the global structure, the circumferential stress in a 90° lamina will be firstly up to the maximum tensile strength of composite lamina as the inner pressure gradually increases. Then the first-ply failure of LCCS will happen. At that time, the inner pressure born by the LCCS is the elastic limit load of structure. By numerical examples, we found that the maximum inner pressure P of LCCS is inversely proportional to the ratio η of the inner radius R_{inner} to the wall thickness $\mathrm{H}_{thickness}$ of cylindrical structure. And $\mathrm{P}=C/\eta$, where C is a constant which is only determined by homogenized stiffness parameters when the strength parameters of composites keep invariable. Table 3 shows the homogenized stiffness parameters of LCCSs made by 5 different arrangements. From the table we can see that different arrangements lead to different equivalent stiffnesses, but both arrangements including [45°/0°/-45°/90°] and [45°/90°/-45°/0°] have the same homogenized parameters. As a result, some relationships between P and η with different arrangements are obtained as illustrated in Fig. 6. Also, as η increases, P decreases. However, because the constants C determined by the homogenized parameters are different, those curves have similar shapes but not coincide each other except [45°/0°/-45°/90°] and [45°/90°/-45°/0°] with the same homogenized parameters. Furthermore, it is worth to pay attention that when η is small ($\eta<5$) there are very small differences between both preceding curves. In fact, the more the number of arrangement periods is, namely the smaller ε relative to the size of the global structure is, the nearer both curves are.

Table 3. Equivalent homogenized mechanical parameters of cylinder in different ply arrangements

Material	Homogenized Stiffness Parameters								
T300/5208	E_1(GPa)	E_2(GPa)	E_3(GPa)	G_{12}(GPa)	G_{23}(GPa)	G_{13}(GPa)	ν_{12}	ν_{23}	ν_{13}
[45°/ 0°/-45°/90°]	12.98	69.68	69.68	4.66	26.89	4.66	0.060	0.296	0.060
[45°/90°/-45°/ 0°]	12.98	69.68	69.68	4.66	26.89	4.66	0.060	0.296	0.060
[45°/90°/-45°/90°]	12.54	103.98	29.22	5.65	26.89	3.97	0.014	0.675	0.169
[45°/ 0°/-45°/ 0°]	12.54	29.22	103.98	3.97	26.89	5.65	0.169	0.190	0.014
[45°/-45°/45°/-45°]	12.98	25.05	25.05	4.66	46.61	4.66	0.060	0.747	0.060

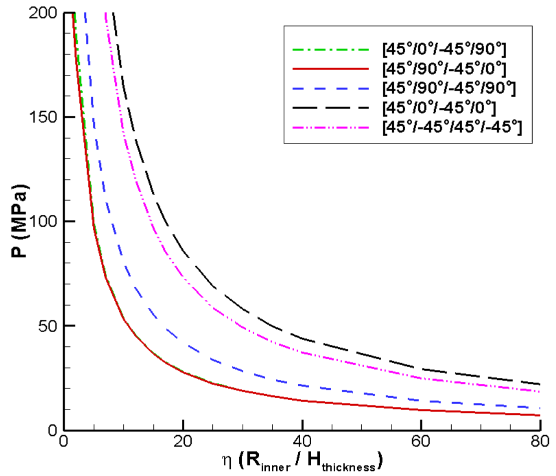

Fig.6. Correlation of the maximum inner pressure with the ratio of the inner radius to the wall thickness of cylinder with different arrangements

Example 2:

For the hollow cylinders subject to linearly varying pressures shown in Section 4.2, the mechanical properties of LCCS are predicted. The structure of cylinder is the same as that in the example 1. In order to reveal results expediently, the length of the cylinder for calculation is 10mm. And the inner pressures are $\mathrm{Pa} = 15\mathrm{MPa}, \mathrm{Pa}^* = 15\mathrm{MPa}$, where the symbols $\mathrm{Pa}, \mathrm{Pa}^*$ are shown in figure 3, the outer pressures are zero. In this example, the strain distributions of cylinder are calculated and the contour plots of stain are displayed. These results predicted by STMCC are compared with other results computed by ANSYS software.

The contour plots of $\varepsilon_r, \varepsilon_\theta, \varepsilon_z$ and γ_{rz} in r-z section are shown from the figure 7 to the figure 10. In each figure, the right plot comes from ANSYS, and the left one is obtained by STMCC. From these figures we can see that the left strain results are very close to the right ones. Furthermore, the stress results also can be obtained by Hooke's Law.

It is worth mentioning that with the number of thin laminas increasing the computing capacity and time of ANSYS software increase sharply, while the STMCC save much of the calculation and computing time in ensuring the precision of results.

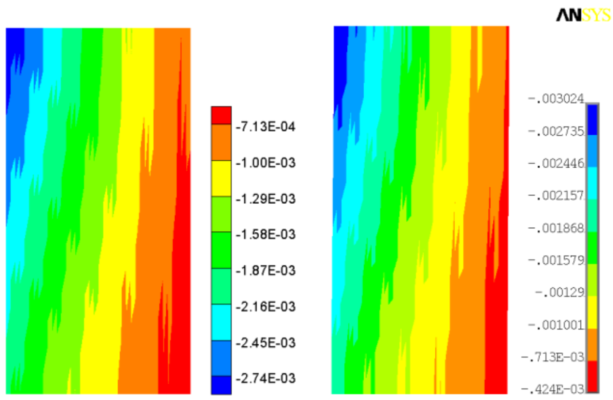

Fig.7. Contour plots of strain ε_r in r-z section

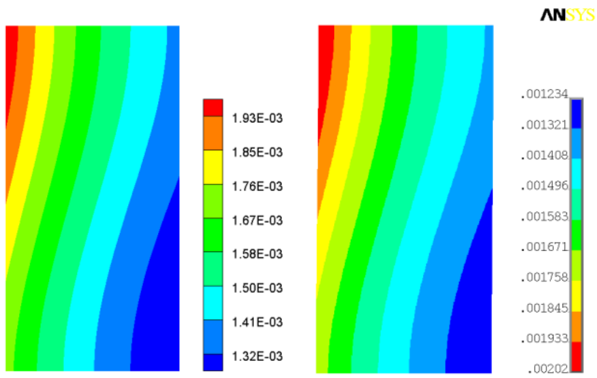

Fig.8. Contour plots of stress ε_θ in r-z section

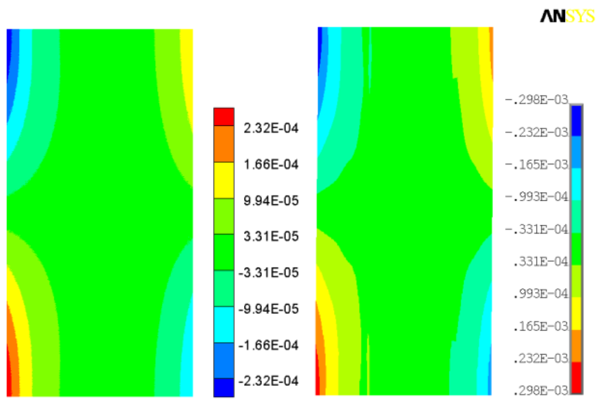

Fig.9. Contour plots of stress ε_z in r-z section

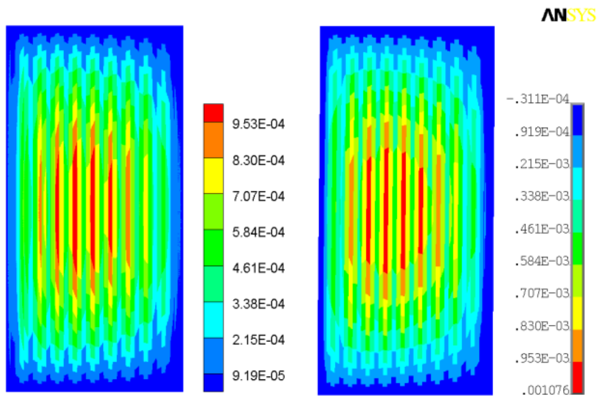

Fig.10. Contour plots of stress γ_{rz} in r-z section

7 Conclusions and Discussion

In this paper, an elasticity system in cylindrical coordinates is derived by defining four different operators and introducing an extended fourth-rank tensor. And then, the Second-order and Two-scale Method in Cylindrical Coordinates (STMCC) is presented for predicting the mechanical properties, including stiffness parameters, strains and stresses and elastic limit loads. For an example of the periodically laminated composite cylindrical structure, its material is homogeneous in circumferential and axial distribution, but periodical in radial direction. So the cell's equation is reduced to one-dimension problem in r direction. Furthermore, by analyzing the numerical results of STMCC, the elastic limit load of LCCS subject to uniform pressure is determined, and is inversely proportional to the ratio of the inner radius to the wall thickness of cylindrical structure, which is instructive for composite structure design.

The numerical examples are only the typical mechanics problems of cylinder with axis-symmetric loads, which often rise in the analysis of pressure vessel or pipeline, etc. But they have shown that the second-order and two-scale method in cylindrical coordinates in this paper is effective for mechanical property prediction of periodically laminated composite cylindrical structures, and the more the composite layers are, the more efficient the second-order and two-scale method is.

Acknowledgements

This work is supported by the Special Funds for Major State Basic Research Project (2005CB321704) and National Natural Science Foundation of China (10590353 and 90405016), and also supported by the center for high performance computing, NWPU in China.

References

[1] I.Babuska, Homogenization and its applications, mathematical and computational problems, Numerical Solutions of Partial Differential Equations-Ⅲ. Academic Press, New York, 1976, 89-116.

[2] A.Bensousson, J.L.Lions, and G.Papanicolaou, Asymptotic Analysis for Periodic Structure, North-Holland, Amsterdam, 1978.

[3] O.A.Oleinik, A.S.Shamaev, and G.A.Yosifian, Mathematical Problems in Elasticity and Homogenization, North-Holland, Amsterdam, 1992.

[4] J.Z.Cui and H.Y.Yang, "A dual coupled method for boundary value problems of PDE with coefficients of small period", Journal of Computational Mathematics, Vol.14, No.2, 1996, 159-174.

[5] J.Z.Cui, T.M.Shin and Y.L.Wang, "Two-scale analysis method for bodies with small period configuration", Invited Paper in CASCM-97, Feb. 11-14, 1997, Structural Engineering and Mechanics, Vol.7, No.6, 1999, 601-614.

[6] Y.Y.Li and J.Z.Cui, "The multi-scale computational method for mechanics parameters of the materials with random distribution of multi-scale grains", Journal of Composites Science and Technology, 65 (2005), 1447-1458.

[7] X.G.Yu and J.Z.Cui, "The prediction on mechanical properties of 4-step braided composites via two-scale method, Journal of Composites Science and Technology, 67 (2007), 471-480.

[8] Y.P.Liang, H.Z.Wang, X.M.Ren, "Analytical solution for spatially axisymmetric problem of open-ended thick-walled cylinder subjected to different linearly varying pressures", Journal of Northwestern Polytechnical University, Vol.24, No.5, 2006, 658-661.

[9] X.S.Lin, "Space axisymmetrical stress analysis of composite thick-wall cylindrical shaft lining of finite length", Journal of China Coal Society, Vol.15, No.4, 1990, 35-45.

[10] L.Parnas, N.Katirci, "Design of fiber-reinforced composite pressure vessels under various loading conditions", Composite Structures, Vol.58, 2002, 83-95.

[11] C.X.Zheng, Composite Pressure Vessels (in Chinese), Chemical Industry Press (in China), 2006.